A cautionary note on quantitative measures of phenotypic convergence

David M. Grossnickle[1*], William H. Brightly[1], Lucas N. Weaver[2], Kathryn E. Stanchak[1], Rachel A. Roston[3], Spencer K. Pevsner[4], C. Tristan Stayton[5], P. David Polly[6], Chris J. Law[7]

[1]University of Washington, Department of Biology
[2]University of Michigan, Department of Ecology and Evolutionary Biology and Museum of Paleontology
[3]University of Washington, School of Dentistry, Department of Oral Health Sciences
[4]University of Oxford, Department of Earth Sciences
[5]Bucknell University, Department of Biology
[6]Indiana University, Department of Earth and Atmospheric Sciences
[7]University of Texas, Austin, Department of Integrative Biology

*Correspondence: dmgrossn@uw.edu

ABSTRACT

Tests of phenotypic convergence can provide evidence of adaptive evolution, and the popularity of such studies has grown in recent years due to the development of novel, quantitative methods for identifying and/or measuring convergence. Two commonly used methods include (i) 'distance-based' methods that measure morphological distances between lineages in phylomorphospace and (ii) fitting evolutionary models to morphological datasets to test whether lineages have evolved toward adaptive peaks. Here, we demonstrate that both types of convergence measures are influenced by the position of putatively convergent taxa in morphospace such that morphological outliers are statistically more likely to exhibit convergence by chance. A more substantial issue is that some methods will often misidentify divergent lineages as being convergent. These issues likely influence the results of many studies, especially those that focus on morphological outliers. To help address these problems, we developed a new distance-based method for measuring convergence that incorporates distances between lineages through time and minimizes the possibility of divergent taxa being misidentified as convergent. We advocate the use of this method when the phylogenetic tips of

putatively convergent lineages are of the same or similar geologic ages (e.g., extant taxa), meaning that convergence among the lineages is expected to be synchronous. We conclude by emphasizing that all available convergence measures are imperfect, and researchers should recognize the limitations of these methods and use multiple lines of evidence when inferring and measuring convergence.

KEYWORDS: convergent evolution, evolutionary models, Ornstein-Uhlenbeck models, phylomorphospace, adaptive evolution

INTRODUCTION

Phenotypic convergence among distantly related taxa is commonly associated with adaptive evolution (e.g., Darwin 1859, Losos 2011), but it can also occur stochastically (Stayton 2008) or as a byproduct of shared developmental constraints (Losos 2011, Speed and Arbuckle 2016). Evidence that convergence is due to adaptation requires showing that the magnitude of convergence is greater than expected by chance, and also that the convergent phenotypes are tied to similar ecological or functional roles. Thus, quantitative examinations of phenotypic convergence are important; they assist researchers in identifying adaptive morphological changes that are driven by shared selective pressures and/or developmental constraints. Novel methods for identifying and measuring convergence have recently been developed (Mahler et al. 2013, Arbuckle et al. 2014, Ingram and Mahler 2013, Stayton 2015A, Speed and Arbuckle 2017, Castiglione et al. 2019), and these methods are often accompanied by statistical tests for comparing the measured convergence to that which is expected from a null model-fitting hypothesis or random data permutations. This has increased the accessibility of quantitative tests for phenotypic convergence, leading to a flood of recent studies on that topic (e.g., Friedman et al. 2016, Zelditch et al. 2017, Da Silva et al. 2018, Arbour and Zanno 2020, Grossnickle et al. 2020, Martinez et al. 2020, Serio et al. 2020, Spear and Williams 2020, Baumgart et al. 2021, Huie et al. 2021, Rovinsky et al. 2021, Tamagnini et al. 2021, Alfieri et al. 2021, Law 2022, Canale et al. 2022).

Phenotypic convergence is often defined as lineages evolving to be more similar to one another than were their ancestors (Losos 2011, Stayton 2015A, Mahler et al. 2017), and we follow that definition here. Thus, a signature of convergence is phylogenetic tips that are phenotypically more similar to one another than expected based on assumptions of random change over time; the degree of this similarity of tips is often quantified by convergence measures (Speed and Arbuckle 2017). However, a confounding issue is that multiple types of evolutionary trajectories can result in lineages that are more similar to one another than expected by chance but are not convergent (as defined above). This includes lineages that retain a shared ancestral morphology (see discussion on 'conservatism' below) and lineages that have parallel evolutionary trajectories from a similar ancestral trait condition.

The *C*1–*C*4 measures (hereafter, '*C*-measures') developed by Stayton (2015A) have emerged as an especially popular means of quantifying phenotypic convergence (e.g., Friedman et al. 2016, Zelditch et al. 2017, Da Silva et al. 2018, Arbour and Zanno 2020, Grossnickle et al. 2020, Martinez et al. 2020, Spear and Williams 2020, Baumgart et al. 2021, Huie et al. 2021, Rovinsky et al. 2021, Tamagnini et al. 2021, Law 2022, Canale et al. 2022). *C*-measures are calculated using geometric distances in phylomorphospace between focal lineages, relying on ancestral reconstructions for morphologies at ancestral nodes. The underlying feature of the *C*-measures is the comparison of two measurements: the maximum phenotypic distance between lineages at any points in their evolutionary histories (D_{max}) and the phenotypic distance between phylogenetic tips (D_{tip}). More specifically, D_{max} is the greatest distance between any two points along the lineages in phylomorphospace, with candidate distances including any points between the lineages' most recent common ancestor and the tips (Fig. 1A). *C*1 is the primary *C*-measure and calculated as $1 - (D_{tip}/D_{max})$, with the resulting value representing "the proportion of the maximum distance between two lineages that has been 'closed' by subsequent evolution" (Stayton 2015A). In our conceptual illustration (Fig. 1A), two lineages have convergently evolved such that their tips are 70% closer to each other than their D_{max}, resulting in a *C*1 score of 0.7.

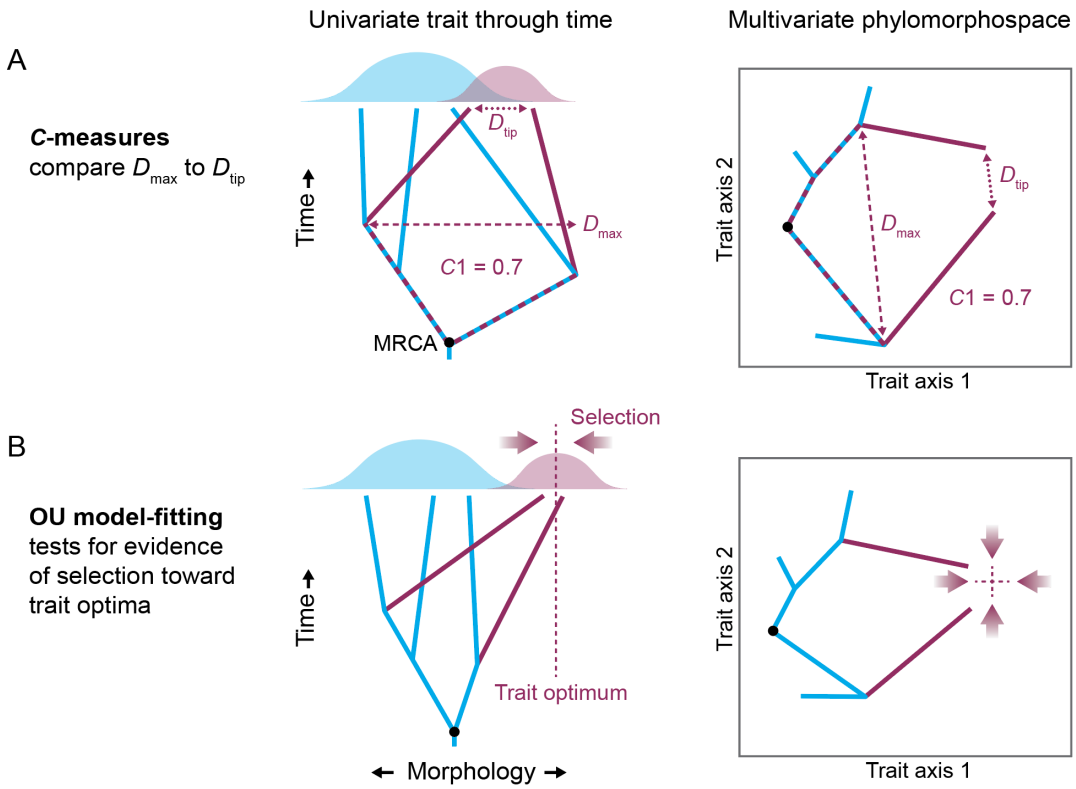

Figure 1. Conceptual illustrations of two methods for assessing phenotypic convergence of focal lineages (maroon): *A*, *C*1 of Stayton (2015A) and, *B*, Ornstein-Uhlenbeck (OU) model-fitting. The *C*1 score of 0.7 indicates that lineages have evolved toward each other to cover 70% of the maximum distance (D_{max}) between their lineages. D_{max} can be measured at any point along the evolutionary histories, including the dashed branches in *A*, and D_{tip} is the morphological distance between phylogenetic tips. Although time is a variable in the univariate illustration in *A*, the *C*-measures do not incorporate time. *B*, OU models include fitting a trait optimum parameter that is often interpreted as the location of an adaptive peak and an 'attraction' parameter that is commonly interpreted as the strength of selection. Abbreviation: MRCA, most recent common ancestor.

One reason for the popularity of *C*-measures is that they can distinguish between convergence and conservatism, which both result in distantly-related phylogenetic tips with similar phenotypes. The key difference between convergence and conservatism centers on the ancestral morphologies of the lineages. Whereas convergence involves ancestors that were less morphologically similar to each other than their descendant tips are to one another (Losos 2011, Stayton 2015A, Mahler et al. 2017), conservatism is the lack of substantial phenotypic divergence from ancestral morphologies relative to

118 what is expected from random processes (Losos 2008, Moen et al. 2013, McLean et al. 2018). The 'blue' lineages in Figure 1B could be considered an example of
120 conservatism; they have not evolved far from the ancestral morphology. *C*-measures account for ancestral patterns via the D_{max} measurement (Fig. 1A). Alternative distance-
122 based methods for testing for convergence (e.g., Wheatsheaf index, Arbuckle et al. 2014, Arbuckle and Minter 2015; θ, Castiglione et al. 2019) cannot adequately
124 differentiate between convergence and conservatism (or parallelism) because phenotypic distances between ancestral morphologies are not considered or, in the
126 case of θ, only partially integrated (Castiglione et al. 2019).

In addition to distance-based measures, researchers often use evolutionary
128 model-fitting analyses to test for convergence, using strong fits of Ornstein-Uhlenbeck (OU) models (Hansen 1997, Butler and King 2004) to morphological data as evidence
130 of convergence (e.g., Mahler et al. 2013, Ingram and Mahler 2013, Friedman et al. 2016, Mahler et al. 2017, Grossnickle et al. 2020, Martinez et al. 2020). An OU process
132 involves 'attraction' toward an 'attractor' or trait optimum (commonly interpreted as the location of an adaptive peak), and this attraction and any resulting convergence is often
134 assumed to be due to selective pressures toward adaptive peaks (Fig. 1B). Convergence is identified when the best-supported model indicates that two or more
136 lineages have independently begun evolving toward the same trait optimum. OU model-fitting analyses may fail to differentiate between convergence and conservatism
138 because conservatism (or long-term stasis) is also an expected outcome of an OU process (Hansen 1997), although in the case of conservatism no switch from an
140 ancestral to derived optimum may be inferred. However, a benefit of OU model-fitting analyses is that the magnitude of the attraction parameter allows an estimate of
142 selective strength toward adaptive peaks, thus providing information about the process that may be driving convergence.

144 Here, we highlight a critical concern with *C*-measures and OU model-fitting analyses: in some circumstances either approach may misclassify divergent lineages as
146 convergent, especially when those lineages are outliers in morphospace. Misclassification occurs for different reasons with each method, but in both cases it is
148 more likely to occur with greater distances between the lineages of interest and their

ancestral morphology (i.e., the lineages are greater morphological outliers). We demonstrate the problem by applying both methods to simulated data in which a subset of lineages are modeled as truly convergent or truly divergent. We also assess other distance-based metrics for measuring convergence and find that θ (i.e., the angle between phenotypic vectors) is also biased toward misclassifying morphological outliers as convergent, whereas the Wheatsheaf index is biased but in the opposite direction, indicating greater convergence among lineages that retain their shared ancestral morphology. Finally, we present an improved method for calculating *C*-measures that minimizes the possibility of erroneously measuring divergent lineages as convergent, which is most applicable to data where the phylogenetic tips are of the same or similar age (e.g., for evaluation of convergence among extant taxa).

METHODS

Evolutionary simulations

We generated a series of simulated trait datasets to ascertain how frequently convergence measures correctly identify *convergent* lineages and misclassify *divergent* lineages as convergent. Simulated datasets are intended to reflect typical empirical datasets, and thus we simulated traits on a phylogenetic tree of extant mammals that is currently being used for empirical research. The sample of extant mammalian species (n = 201) builds on the samples in Grossnickle et al. (2020), Weaver and Grossnickle (2020), and Pevsner et al. (2022). We obtained 1000 randomly chosen phylogenetic trees from the posterior distribution of Upham et al.'s (2019) 'completed trees' analysis. We then used *TreeAnnotator* (Drummond et al. 2012) to generate a maximum clade credibility tree, which was pruned to the species in our sample. The sample includes 13 gliding-mammal species representing five independent evolutionary origins of gliding behavior. We treated the gliders as the focal lineages (*sensu* Grossnickle et al. 2020); they were the subject of manipulation in our simulations (as such, we refer to those simulated glider data as 'gliders'). The five 'glider' clades are spread across the mammalian phylogeny and have varying evolutionary origin ages, making them ideal for representing typical empirical datasets.

For each simulated trait set, six traits were evolved by Brownian motion (BM) on all ‘non-glider’ branches to produce a "base tree" using the *SimulateContinuousTraitsOnTree* function in the *Phylogenetics for Mathematica* package (Polly 2019). (Note that the phylogeny is the same for each base tree; only the simulated traits vary with each base tree.) The ancestral value for each trait was arbitrarily set to 0.0 and the step rate, σ^2, was set at 1.0 per million years. Phylogenetic branches of ‘gliders’ were those tipped by one of the 13 ‘glider’ species, plus the subtending branches below clades whose tips were all ‘gliders.’ From the ancestral value generated by BM, the traits on the ‘glider’ branches were systematically selected toward varying trait optima (see below) using an OU model. Selection toward optima was simulated using the *LineageEvolution* function in *Phylogenetics for Mathematica*.

For convergence simulations, the traits simulated to be convergent (of the six traits) were all selected toward the same trait optimum. The selected branches were simulated for their full duration, which allowed all but the shortest branches to arrive at the adaptive peak. Using the same base tree, each simulation was repeated with a different number of convergent traits: three, four, five, and six. Traits not selected to be convergent were evolved by BM. Each of these was then iterated for a series of 11 trait optima at successively greater distances from the ancestral point in morphospace, starting at 0 (convergence toward the ancestral trait values) and increasing by 10s to a distance of 100 trait units from the ancestral value. For instance, in a simulation with four convergent traits and an optimum of 30, the first four traits all evolved toward an optimum trait value of 30 and the two remaining traits evolved by BM. The range of tip values in the base tree has a radius of about 20 trait units, so the first three optima in this iteration (0, 10, 20) lie within the morphospace occupied by 'non-glider' taxa and the last seven lie increasingly outside the range of morphology of 'non-gliders.' Each simulation with all of its iterations was repeated with 15 unique base trees, and we report results for the means and standard errors of these 15 replicates.

We simulated divergence among 'glider' lineages in two ways. First, we simulated divergence as occurring via drift, using a BM process. Six traits were simulated using the *fastBM* function of the *phytools* package (Revell 2012) for *R* (*R* Core Team 2020). Ancestral trait values were set at zero, and, to mimic natural

variation, the rate parameter (σ^2) was sampled from a log-normal distribution with log-
212 mean and standard deviation 0 and 0.75, respectively. This was repeated to produce 15 replicate datasets. Second, we simulated divergence as selection of the individual
214 'glider' lineages each toward a different trait optimum using a procedure that is as parallel as possible to that used in the convergence simulations. Between three and six
216 traits were selected toward the clade-specific trait optimum with a series of target distances ranging from 30 trait units from the ancestral morphology (which extends the
218 lineages past the periphery of the base BM tree and thus ensures that the targets are divergent) to 100 units in steps of 10. This choice, however, means that the divergence
220 simulations are limited to cases in which the lineages are morphological outliers (i.e., they evolve beyond 20 trait units), whereas the drift-based divergence simulations
222 include non-outlying lineages. A different target was randomly selected for each 'glider' clade by choosing a random positive trait value for each of the traits under selection
224 with the condition that their sum of squares equal the squared target distance (i.e., that the target lies at a distance of 30, 40, etc. units from the ancestral trait values).
226 Choosing only positive trait values ensures that the lineages are allowed to diverge in fully multivariate directions yet lie within the same multidimensional 'quadrant.' The
228 selected lineages are allowed to fully reach their trait optima.

In total, we generated and analyzed 1,155 simulated datasets: 660 that simulated
230 trait convergence and 495 that simulated trait divergence.

232 ***C*-measures**

We applied the *C*-measures (Stayton 2015A) to focal lineages (‘gliders’) in the
234 simulated datasets. The primary measure, *C*1, is the distance between phylogenetic tips of focal taxa (D_{tip}) divided by the maximum distance between any tips or ancestral
236 nodes of those lineages (D_{max}). The resulting proportion is subtracted from one; the *C*1 value is one for complete convergence zero for divergence (i.e., D_{max} is D_{tip}). *C*2 is D_{max}
238 subtracted by D_{tip}, and it captures the absolute magnitude of convergent change. *C*3 and *C*4 are standardized versions of *C*2 that are calculated by dividing *C*2 by the
240 phenotypic change along branches leading to the focal taxa (*C*3) or the total amount of phenotypic change in the entire clade (*C*4). See Stayton (2015A) for full descriptions of

242 *C*1–*C*4. To calculate *C*-measure scores, we used functions in the *R* script from Zelditch et al. (2017), which are computationally faster than the functions in the *convevol R*
244 package (Stayton 2015A, Stayton 2018). Due to computational limits of analyzing a large number of simulated datasets, we only calculated simulation-based *p*-values for a
246 smaller subset of datasets used for subsequent analyses (see the following subsection).

C-measures quantify phenotypic convergence between individual phylogenetic
248 tips, not between clades with multiple tips (Stayton 2015A). Thus, we calculated average phenotypes for taxa of focal clades. For example, one glider clade includes six
250 flying squirrel species, so for each of the six simulated traits we calculated mean values for the six species. The averages were then used as the representative flying squirrel
252 lineage. Thus, *C*-measures were measured for five 'glider' lineages, each representing an independent evolution of gliding. The species' traits were not averaged prior to the
254 other types of convergence analyses described below.

256 **Additional measures of convergence**

Subset of simulated datasets. We applied additional measures of convergence (OU
258 model-fitting, θ, and Wheatsheaf index) to a smaller subset of 30 simulated datasets. This subset only includes datasets in which four of six traits were simulated to converge
260 on a specific trait optimum or diverge toward multiple optima, with the remaining two traits evolved by BM (see Evolutionary simulations subsection for more details). We did
262 not use datasets in which all six traits are convergent because this leads to nearly complete convergence on a trait optimum, and complete convergence appears to be
264 very rare among empirical analyses (Grossnickle et al. 2020). Nonetheless, four of six traits being convergent on an optimum often results in strong convergence (i.e.,
266 statistically significant distance-based measures of convergence and strong fits of multiple-peak OU models) among lineages, especially when trait optima are outliers in
268 morphospace (see Results & Discussion). For convergence simulations, we randomly chose five simulated datasets each from the sets of simulations where trait optima were
270 set at 0, 20, 50, and 100. These represent simulations in which focal lineages evolve toward the ancestral morphology (optimum = 0), evolve to the outer edge of the
272 morphospace region of BM-evolved lineages (optimum = 20), and evolve far into

outlying morphospace (optima = 50 and 100). For divergence simulations, we randomly
274 chose five simulated datasets each with optima of 50 and 100. (Using trait optima of 0
or 20 could mistakenly simulate convergence toward ancestral morphologies.) Thus, the
276 subset of datasets includes 20 convergence simulations (five datasets each for four trait
optima) and 10 divergence simulations (five datasets each for two optima). The
278 following methods were only applied to this subset of 30 datasets.

Evolutionary model-fitting analyses. We fit three multivariate models to all six
280 simulated traits using functions within the *mvMORPH R* package (Clavel et al. 2015).
The first two models were a single-rate multivariate BM model (mvBM1) that assumes
282 trait variance accumulates stochastically but proportionally to evolutionary time, and a
single-optimum Ornstein-Uhlenbeck model (mvOU1) that modifies the BM model to
284 constrain each trait to evolve toward a single optimum. Support for mvBM1 or mvOU1
would indicate a lack of strong convergence among the taxa simulated as convergent or
286 divergent, due to the lack of evidence for a distinct adaptive peak associated with
'gliders.' We then fit a multivariate OU model with two selective regimes (mvOU2) that
288 allowed 'gliders' and 'non-gliders' to exhibit different trait optima (θ). Support for mvOU2
would provide evidence of convergence by indicating that selective forces are driving
290 'glider' lineages to a shared adaptive peak (Fig 1B). Note that the simulations evolved
'non-gliders' via BM, and thus any support for the mvOU2 model is likely to be driven by
292 the 13 'glider' lineages. Although we generated the datasets and thus could use the
known ancestral character states of each dataset, our goal is to treat the data like an
294 empirical dataset with unknown ancestral states. Thus, we stochastically mapped
ancestral character states on each tree as 'simmaps' (Bollback 2006), and to account
296 for ancestral state uncertainty we used 10 'simmaps' for each of the 30 datasets (six
sets of five datasets). Relative support for each of the three models was assessed
298 through computation of small-sample corrected Akaike weights (AICcW; Akaike 1974;
Hurvich and Tsai 1989). For each set of five datasets, we calculated AICcW for each of
300 the 50 total trees (five datasets with 10 'simmaps' each), and we report the mean values
for these trees.

302 As a supplemental analysis, we fit models to univariate data (PC1 scores) using
functions in the *OUwie R* package (Beaulieu et al. 2012). This includes multiple-regime

304 OU models that permit evolutionary rates (σ) and/or attractions to optima (α) to vary
between regimes, which is not a feature of the multivariate *mvMORPH* models. See the
306 Supplemental Methods for additional information.

Additional distance-based convergence measures. We applied two other
308 measures of convergence to the subset of 30 simulated datasets (using all six traits):
Wheatsheaf index, which was implemented via the *R* package *windex* (Arbuckle et al.
310 2014, Arbuckle and Minter 2015), and θ_{real}, which was implemented using the *RRphylo*
package (Castiglione et al. 2018, Castiglione et al. 2019). The Wheatsheaf index
312 measures pairwise morphological distances between putatively convergent taxa, with
distances corrected for the degree of phylogenetic relatedness of lineages. These
314 distances are compared to pairwise distances between other lineages in the sample to
determine whether putatively convergent lineages are more similar to each other than
316 expected. The θ measurement is the angle between the phenotypic vectors of putatively
convergent lineages (note that this θ is different from the θ parameter of OU models),
318 and it is based upon phylogenetic ridge regression. We report the angle obtained by all
pairwise comparisons between putatively convergent clades (θ_{real}), standardized by the
320 phylogenetic distance separating them (i.e., expected divergence under a BM model).
Significance tests compare standardized θ_{real} values of putatively convergent taxa to
322 values computed for randomly selected tip pairs.

324 RESULTS & DISCUSSION

326 *C*-measure issues

Our analysis of the *C*-measure calculations reveals that the measures do not always
328 perform as intended (Stayton 2015A), especially when putatively convergent lineages
are outliers in morphospace. This critical problem can manifest in at least three ways,
330 which we illustrate in Figure 2. First, the more outlying the morphologies are in
phylomorphospace (and all else being equal), the greater the *C* scores, indicating
332 stronger convergence. We demonstrate this with a conceptual illustration in Figure 2A
(note that D_{tip} remains constant in both scenarios). This does not align with the working
334 definition of convergence used in this study and in Stayton (2015A); the distances

between ancestral nodes and the distances between descendants are unchanged
336 between the scenarios, and thus we could expect *C* scores to be the same for both
scenarios. The pattern of greater convergence in outliers is also demonstrated by
338 results of applying *C*-measures to evolutionary simulations (Figs. 3 and S1); taxa
evolving to trait optima farther from the ancestral morphology have greater *C*1–*C*4
340 scores. The only exception is the *C*1 set of results when all six simulated traits are
convergent. In this case, *C*1 scores remain consistently around 0.8 regardless of the
342 position of trait optima (Fig. 3C).

344

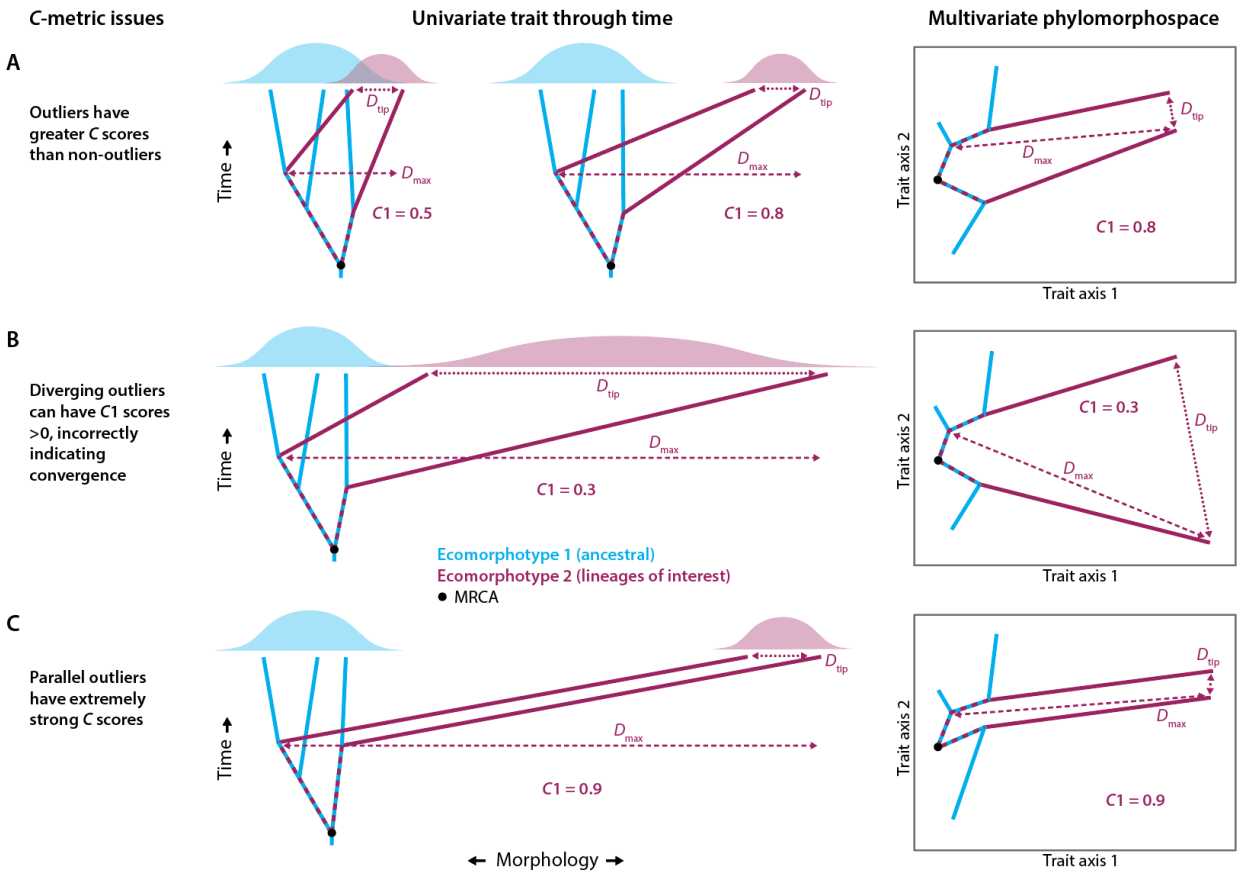

346 **Figure 2**. Conceptual illustrations of *C*-measure issues. *C*1 scores are greater than zero for
the divergent (*B*) and parallel (*C*) lineages (Ecomorphotype 2), incorrectly indicating that the
348 lineages are convergent. See the main text and Figure 1 for more information on *C*1, D_{max},
and D_{tip}. The *C*-measure issues highlighted here also apply to evolutionary model-fitting
350 analyses. The distribution curves in univariate illustrations could represent adaptive peaks,
and OU model-fitting analyses are more likely to identify unique adaptive peaks when a
352 peak is farther from the ancestral morphology (Table 1).

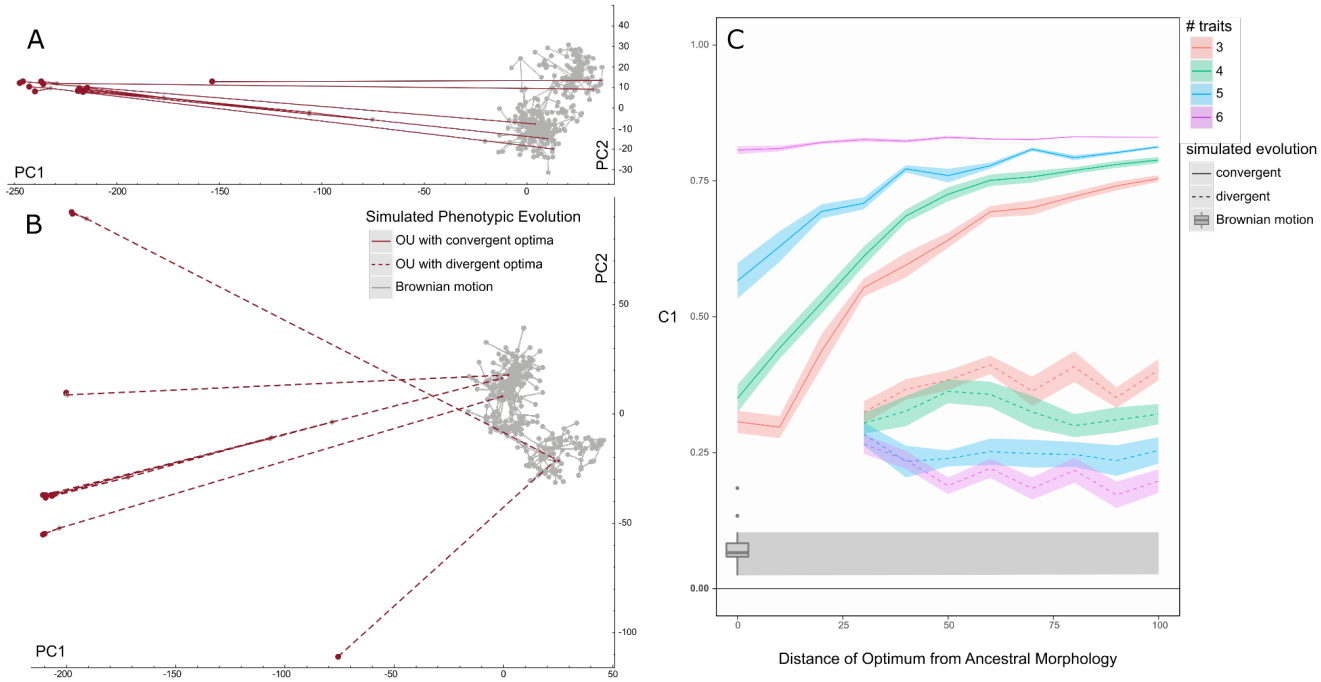

Figure 3. PCA phylomorphospaces for example datasets that simulate convergence (*A*) and divergence (*B*) of all six traits of five focal taxa ('gliders'). Traits were selected toward optima via an OU process, with all traits of convergent taxa selected toward a value of 100 and traits of divergent taxa selected toward varying values that result in evolutionary change equal to that of convergent taxa (see Methods). (*C*) *C*1 scores for simulated convergent lineages (solid lines) and divergent lineages (dashed lines), using datasets in which focal taxa have varying numbers of convergent/divergent traits (of six total) and trait optima positions. Any traits and lineages not selected to be convergent/divergent were evolved by Brownian motion (BM). Focal taxa evolved toward trait optima after they originated. Divergent trait optima are randomized, but they are limited to being positive numbers (whereas BM-evolved traits can be positive or negative), resulting in divergent lineages evolving in the same direction along PC1 (e.g., *B*) but otherwise being divergent (unless convergence occurs by chance). *C*1 values above zero indicate convergence, and a value of one would reflect complete convergence (i.e., phenotypically identical tips). We did not simulate divergence to trait optima of 0, 10, and 20 because the simulations might mistakenly generate convergent lineages near the middle of morphospace. As a second means of simulating divergence, we allowed the focal lineages to evolve via BM, and these results are displayed as a box-and-whisker plot in *C*. *C*1 results are means and standard errors of 15 simulated datasets.

The second and third issues with the *C*-measures are more problematic: divergent and parallel lineages can have *C*1 scores that are greater than zero, incorrectly indicating that the lineages are convergent (Fig. 2B, C). In Figure 2B we illustrate lineages that are diverging morphologically (in univariate and multivariate morphospace), but they have a *C*1 score of 0.3, incorrectly suggesting that the lineages have experienced substantial convergence (i.e., closing about 30% of the maximum distance between lineages). To further test this issue, we measured *C*1 in lineages simulated to have divergent traits (Fig. 3B), and *C*1 values are consistently greater than zero (Fig. 3C), incorrectly indicating convergence instead of divergence. This has major implications for empirical studies (see discussion of examples below); divergent lineages may often be incorrectly interpreted to be convergent.

Similarly, outlying lineages evolving along parallel phylomorphospace trajectories from a similar ancestral condition have extremely strong *C*1 scores (Fig. 2C). This is unexpected because the ancestral nodes of both lineages are the same morphological distance from one another as the distance between tips; this is not convergence according to the definition of convergence adopted here or in Stayton 2015A (see Introduction; Losos 2011, Mahler et al. 2017).

The possibility of diverging and parallel lineages having *C*1 scores that incorrectly indicate convergence (i.e., are greater than zero) stems from the D_{max} measurement (as defined by Stayton 2015A and calculated in versions 1.0 through 1.3 of the *convevol R* package), which can be erroneously inflated, especially when lineages are morphological outliers. D_{max} can be measured between ancestral nodes (e.g., see the illustration in Figure 1A), between tips, or between a node and a tip (which is the case in all examples in Figure 2). For converging lineages, D_{max} is expected to be longer than D_{tip} (Stayton 2015A). For diverging lineages, in contrast, D_{max} is expected to be the morphological distance between the tips, meaning that D_{max} equals D_{tip} (and *C*1 = 0). However, this is not always the case; divergent lineages can have a D_{max} length that is not between tips, as illustrated in Figure 2B. Thus, D_{max} can be greater than D_{tip} (indicating convergence) even when lineages are divergent. Although we illustrate this issue using diverging phylogenetic tips (Fig. 2B), the problem could also arise if there

are internal nodes that are similarly divergent and outlying in morphospace (and branching lineages from those nodes do not converge on other focal lineages); thus, this issue is not solely due to allowing D_{max} to be measured to tips.

Other measures of convergence show biased results

Distance-based convergence measures. To test whether other convergence measures also experience similar issues as those of the *C*-measures, we applied two other 'distance-based' metrics (Wheatsheaf index [Arbuckle et al. 2014, Arbuckle and Minter 2015] and θ [Castiglione et al. 2019]) and OU model-fitting analyses to a subset of simulated datasets (Table 1).

Table 1. Tests of convergence among focal lineages of the simulated datasets using distance-based measures. Results are means of five randomly chosen simulated datasets for each optimum. For θ results, we report θ_{real} standardized to phylogenetic distance between clades. Note that relatively smaller θ_{real} values (i.e., smaller angles between phenotypic vectors) suggest greater convergence, whereas relatively larger Wheatsheaf index, *C*1, and *Ct*1 values indicate greater convergence. Statistical significance (*, $p \leq 0.05$; **, $p \leq 0.01$; ***, $p \leq 0.001$) for *C*1 and *Ct*1 is based on comparisons to results of 100 simulations via a BM model, and for the Wheatsheaf index it is based on bootstrapping with 1000 replicates. Significance of standardized θ_{real} values is based on bootstrapping with 1000 replicates for each pairwise comparison between the five 'glider' clades (except the monospecific clade). In all cases, the reported significance is based on means of all analyses for a given trait optimum.

	Convergence measure	Trait optimum			
		0	20	50	100
Convergence simulations	θ (*RRphylo*)	0.329	0.137	0.068**	0.029**
	Wheatsheaf index	1.900***	1.77***	1.043	0.434
	C 1	0.365***	0.559***	0.702***	0.805***
	Ct 1	0.183**	0.233***	0.442***	0.559***
Divergence simulations	θ (*RRphylo*)	–	–	0.269	0.267
	Wheatsheaf index	–	–	0.620	0.344
	C 1	–	–	0.349***	0.298*
	Ct 1	–	–	-0.013	-0.029

Consistent with the *C*-measures, the θ_{real} results (standardized to phylogenetic
438 distance between clades) indicate greater convergence in morphological outliers (Table
1). That is, the angle between phenotypic vectors, θ_{real}, decreases when lineages
440 evolve toward optima that are farther from the ancestral morphology. This is
unsurprising because a relatively farther trait optimum results in greater trait values in
442 the lineages simulated to be convergent, and, all other variables being equal, greater
trait values should result in smaller angles between phenotypic vectors. However, unlike
444 the *C*-measures, θ_{real} does not identify simulated divergent lineages as convergent
(Table 1).

446 In contrast to the *C*-measures and standardized θ_{real}, the Wheatsheaf index
measures less convergence in outliers relative to non-outliers; values decrease when
448 convergent taxa are farther from the ancestral morphology in morphospace. The
Wheatsheaf index compares the distances between putatively convergent taxa to
450 distances between other tips. Our simulations did not allow all convergent lineages to
completely reach trait optima (Fig. 3A), and for the subset of datasets used for
452 Wheatsheaf index analyses, two of the six simulated traits evolved via BM. Together,
these two factors mean that simulated convergent lineages did not completely converge
454 on a morphology, and the pairwise distances between many tips of simulated
convergent lineages are farther apart from each other than are the pairwise distances
456 between other, BM-evolved lineages (see the phylomorphospace in Figure 3A, but note
that the plot is for data in which all six traits were convergent). If we allowed simulated
458 lineages to completely reach trait optima, then this trend of less convergence in outliers
(as measured by the Wheatsheaf index) might disappear. However, complete
460 convergence on morphologies seems especially rare in empirical datasets (Grossnickle
et al. 2020); thus, we believe that the Wheatsheaf index is likely to show reduced
462 measures of convergence in morphological outliers of most empirical samples, in line
with our simulation results.

464 *Evolutionary model-fitting analyses*. Model support for multiple-regime OU
models is often interpreted as evidence for convergence (Fig. 1B), and our model-fitting
466 results (Table 2) highlight two pitfalls of that assumption. First, for simulated
convergence datasets, the null model representing a lack of convergence, mvBM1 (a

uniform BM model), is the best-fitting model when the trait optimum is zero (i.e., 'gliders' converge on the ancestral morphology). And mvBM1 performs well (mean AICcW of 0.40) when the trait optimum is 20, which simulates convergent lineages evolving to the edge of the central-morphospace 'cloud' of BM-evolved lineages. Model support for mvOU2 strengthens when lineages evolve farther from the ancestral morphology, with an average AICcW of 1.0 for mvOU2 when trait optima are 50 and 100 (Table 2). Thus, OU model-fitting analyses may struggle to identify convergence when lineages converge on a morphology that is similar to the ancestral morphology, and, like *C*-measures and standardized θ_{real}, they may be biased toward measuring stronger convergence when lineages evolve farther from the ancestral morphology.

Table 2. Tests of convergence among lineages of the simulated datasets using evolutionary model-fitting analyses. Model-fitting results for each trait optimum are the mean AICcWs of 50 phylogenetic trees (five datasets with 10 'simmaps' each). Model support for the two-regime model (mvOU2) represents support for convergence because this model reflects evolution of focal lineages toward a shared adaptive peak. Abbreviations: AICcW, small-sample corrected Akaike weights; mvBM, multivariate Brownian motion model; mvOU, multivariate Ornstein-Uhlenbeck model.

	Model	**Trait optimum**			
		0	**20**	**50**	**100**
Convergence simulations	mvBM1	0.991	0.400	0.000	0.000
	mvOU1	0.000	0.000	0.000	0.000
	mvOU2	0.009	0.600	1.000	1.000
Divergence simulations	mvBM1	–	–	0.000	0.000
	mvOU1	–	–	0.000	0.000
	mvOU2	–	–	1.000	1.000

Second, for divergence simulations, the two-regime model (mvOU2) is the best-fitting model (Table 2); this model treats divergent taxa ('gliders') and BM-evolved lineages ('non-gliders') as the two selective regimes. In light of the assumption that support for multiple-regime OU models is evidence of convergence, this result is surprising because the divergent lineages show considerable divergence in

phylomorphospace (Fig. 3C) rather than attraction toward one part of the morphospace (a presumptive adaptive peak, which is an assumption of the OU process). Further, taxa representing the second regime were evolved by BM, not an OU process. Thus, taxa of neither selective regime are expected to be well-fit by by an OU model, and yet the two-regime OU model is a substantially better fit to the data than the null, BM1 model (AICcW for mvOU2 is 1.0 for optima of 50 and 100; Table 2). This indicates evidence of two adaptive peaks, one for 'gliders' and one for 'non-gliders,' even though neither of those groups was simulated as evolving toward an adaptive peak.

A probable explanation for the relatively strong fits of two-regime OU models to divergence datasets is that none of the fitted models are a good fit. The two-regime OU models may simply be the best-fitting of bad-fitting models. Further, multiple-regime OU models are often incorrectly favored over simpler models (Cooper et al. 2016), especially when sample sizes are small, and this may be the case with our divergence datasets. Cooper et al. (2016) suggest examining the phylogenetic half-lives ($\ln(2)/\alpha$) of traits as a measure of the strength of an OU process. To examine this for our datasets, we performed supplemental analyses in which we fit univariate, two-regime OU models that permit the α value parameter to vary between regimes (see Supplemental Methods), which then allows us to calculate the phylogenetic half-life specifically for the 'glider' regime. For simulations with divergent trait optima of 100, the fitted α value (mean of 50 trees) of the best-fitting univariate model (OU2VA; Table S1) to PC1 scores indicates a phylogenetic half-life for the simulated gliders of 35 million years. Three of the five glider clades originated less than 35 million years ago. Thus, the relatively long half-life suggests an especially poor fit of the OU2VA model to the data, despite this model being a better fit than the BM1 and OU1 models according to the AICcW comparisons. Considering that empirical datasets often include complex evolutionary patterns and small sample sizes for some regimes, researchers should be cautious both when choosing models to fit to data and when interpreting results (Cooper et al. 2016). Although not explored in this study, multiple-regime BM (BMM) models may offer alternative options that complement multiple-regime OU models. BMM models allow varying phylogenetic means among regimes and can be fit using functions within some *R* packages, including *mvMORPH* (Clavel et al. 2015). Because BMM models do not

model selection toward an optima, support for BMM models over OUM models may suggest that there is limited or no convergence among lineages of interest (e.g., Grossnickle et al. 2020), and in some cases a BMM model might serve as a more appropriate null model than BM1.

A second factor that may help to explain the relatively strong fits of two-regime OU models to the simulated divergence datasets is that the divergent lineages all remain in the same side of the morphospace (e.g., all divergent lineages are in negative PC1 space in Figure 3B) because we limited optima to be positive values rather than positive or negative (see Methods). Therefore, the lineages may be modeled as evolving toward an especially broad adaptive peak that occupies a large region of morphospace. Figure 2B provides a conceptual illustration of this scenario; the Ecomorphotype 2 lineages are diverging but still appear to be evolving toward a broad adaptive peak, which is broader than the adaptive peak of the ancestral lineages (Ecomorphotype 1). This could be a similar scenario to the divergent outlier lineages in our simulated dataset (Fig. 3C).

Although results of both *C*-measures and OU model-fitting analyses can incorrectly suggest that divergent lineages are convergent, the reasons for this issue are different for the two methods; they are fundamentally different in how they test for convergence. Stayton (2015A, 2015B) highlighted that distance-based measures rely on a pattern-based definition of convergence that does not assume a specific mechanism is driving convergence (although see Mahler et al. 2017 for an opposing view), whereas OU model-fitting analyses assume that a specific mechanism, selective pressure (modeled as the α parameter), is driving convergence, and thus rely on a process-based definition of convergence. A further distinction between these types of convergence measures is that distance-based measures assess *morphological convergence of lineages* (i.e., the focus is on whether lineages are evolving toward each other), whereas OU model-fitting analyses test for *convergence on a morphology* (i.e., the focus is on whether lineages are evolving toward a trait optimum or adaptive peak, not toward each other). This distinction between these two types of convergence measures is important: OU model-fitting analyses are not testing for similarities of lineages but rather similarities of lineages to a morphology; thus, they are less directly

testing for convergence compared to distance-based measures, at least when using the convergence definition followed in this paper.

In sum, all convergence measures show some bias, especially when examining morphological outliers, albeit for different underlying reasons for each method. *C*-measures, θ, and OU model-fitting analyses all result in stronger measures of convergence when simulated convergent taxa evolve toward relatively farther trait optima, and *C*-measures often misidentify divergent lineages as being convergent (Fig. 3C, Table 1). Further, model support for multiple-regime OU models, which is often interpreted as support for convergence, can be misleading because in some scenarios these models may be the best fits to divergent lineages (Table 2). In contrast, the Wheatsheaf index shows weaker convergence in outliers, although the magnitude of this bias may be influenced by our simulation methods (Table 1).

Measuring convergence through time via *Ct*-measures

Despite any shortcomings, *C*-measures have benefits over other convergence measures, including the ability to distinguish between convergence and conservatism (Stayton 2015A). Thus, our objective is not to discourage the use of distance-based metrics like *C*-measures but rather to identify issues and encourage the development of improved measures.

We help to address the *C*-measure issues by presenting novel distance-based convergence measures that are derived from the *C*-measures. The new measures are calculated using the same equations as those for *C*1–*C*4 (except with a change to *C*4; see below and Supplemental Methods), but we limit the candidate D_{max} measurements to distances between lineages at synchronous 'time slices' coinciding with internal phylogenetic nodes. For this reason, the new measures require the input tree to be time calibrated. We refer to the new measures as *Ct*-measures (or *Ct*1–*Ct*4) and D_{max} as $D_{max.t}$ because time (*t*) is incorporated when measuring morphological distances between lineages, unlike the *C*-measures. *Ct*1 scores can be interpreted in the same way as *C*1 scores were intended to be interpreted (Stayton 2015A): positive *Ct*1 scores represent a proportion of the maximum morphological distance between lineages that has been covered by convergent evolution, with a result of one representing complete

convergence. Like *C*-measures, statistical significance for *Ct*-measures is based on comparison with expectations for evolution proceeding entirely on a BM model, with simulations used to generate the expectations.

By limiting the candidate $D_{max.t}$ measurements to time slices, the *Ct*-measures minimize the possibility of $D_{max.t}$ being erroneously inflated by divergent tips. This is conceptually illustrated in Figures 4A and 4B, which are the same scenarios as in Figure 2A and 2B. Whereas the *C*1 score in Figure 2B incorrectly indicates convergence (i.e., *C*1 is greater than zero), the *Ct*1 score in Figure 4B correctly indicates divergence (i.e., the value is negative; unlike the *C*-measures, the *Ct*-measures allow divergence results to be negative).

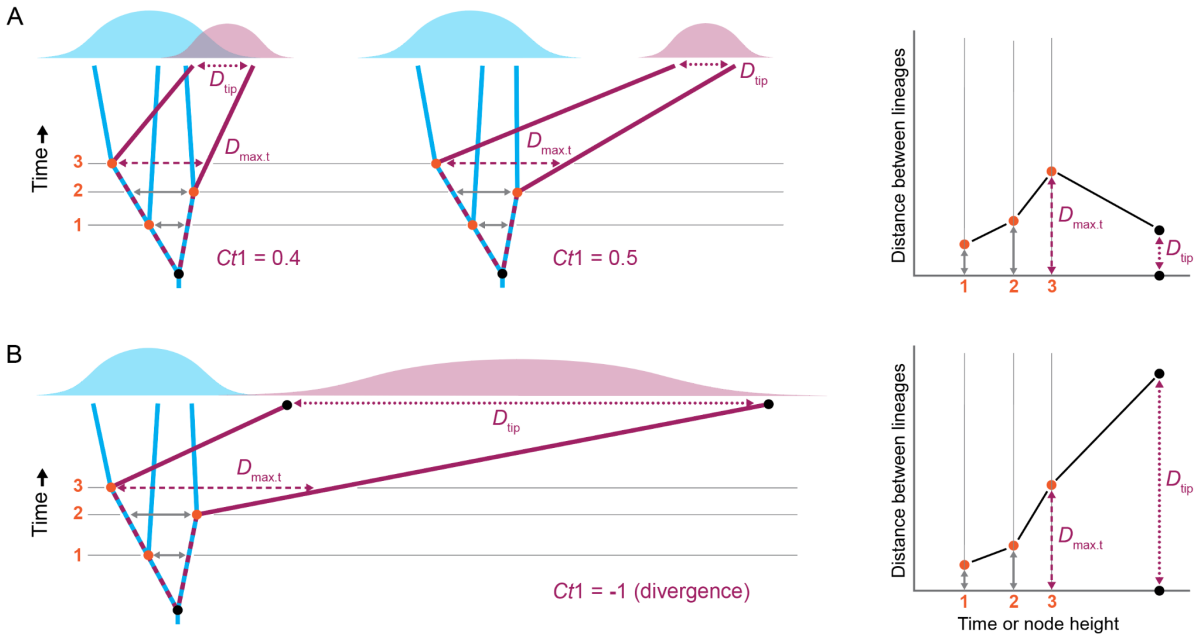

Figure 4. Conceptual illustration of our new *Ct*1 convergence measure, which is calculated like *C*1 of Stayton (2015A) but candidate $D_{max.t}$ measurements are limited to 'time slices' at internal phylogenetic nodes. The plots on the right show the three candidate $D_{max.t}$ measurements and the distance between lineages at the tips (D_{tip}). The scenarios in *A* and *B* are the same as those in Figures 2A and 2B, respectively. In contrast to *C*1, *Ct*1 correctly identifies divergence (negative score) in the scenario in *B*. Although the *Ct*1 score is greater when lineages are outliers (*A*), note that the *Ct*1 scores (0.4 for non-outliers and 0.5 for outliers) are more similar to each than are the *C*1 scores in the same scenarios (0.5 and 0.8; Fig. 2A), indicating that *Ct*-measures are less influenced by positions of taxa in morphospace compared to *C*-measures.

Unlike the D_{max} measurement, the D_{tip} measurement has not been altered from its original implementation in *C*-measures (Stayton 2015A) and is not limited to a synchronous time slice, thus allowing for distances between tips to be compared even if the tips vary in geologic age (e.g., comparison of an extinct taxon and an extant taxon). However, unlike the *C*-measures, the *Ct*-measures do not allow $D_{max.t}$ to be measured between tips (i.e., $D_{max.t}$ cannot equal D_{tip}). This means that divergent taxa will have negative *Ct* scores, whereas *C*-measures (as they were initially intended) will measure divergent taxa as having scores of zero (i.e., D_{max} equals D_{tip}). See the Supplemental Methods for more information on the *Ct*-measures.

In addition to developing the *Ct*-measures, we added several new features to the *convevol R* package (Stayton 2018). This includes allowing *Ct*-measures to compare clades that contain multiple lineages, whereas the *C*-measures are limited to comparisons of individual lineages (see Methods). Clade comparisons are enabled by 1) excluding pairwise comparisons between within-clade lineages (e.g., two flying squirrel species) and 2) weighting of *Ct* scores and *p*-values based on the number of pairwise comparisons between focal clades (see Supplemental Methods). Further, *Ct*-measures can be measured using single traits (*C*-measures only permitted measures of multivariate distances, although they were adapted for univariate analyses in some studies; Spear and Williams 2020, Law 2022), and we updated the *C*4 (now *Ct*4) calculation to better match the original description of that measure. See the Supplemental Methods for additional information on these updates. We used the *R* script from Zelditch et al. (2017) as a foundation for the updated functions. The run times for the revised *R* functions (*convrat.t* and *convratsig.t*) are approximately ten times faster than the original functions of Stayton (2015A) when using our simulated dataset. We did not revise *C*5, which is a frequency-based convergence measure that tallies the number of times lineages enter a region of morphospace (Stayton 2015A), because it is not influenced by the issues highlighted here.

We have also developed a new *R* function, *plot.C*, that produces a plot of the distances between lineages through time. This type of plot is conceptually illustrated in Figure 4, and Figure 5B includes a phylogeny and plot produced by the *plot.C* function for an example dataset from our convergence simulations, showing pairwise distances between three 'glider' lineages. An additional example output of *plot.C* is provided in Figure S5 for the 'twig' ecomorphotype lineages of anoles, although we separated convergent and non-convergent pairwise comparisons for ease of interpretation. These plots allow researchers to visualize when the measured $D_{max.t}$ occurred during the evolutionary history of the lineages, and they may be useful for applications beyond studies of convergence. The candidate $D_{max.t}$ measurements at time slices are provided as an output of the *convrat.t* function.

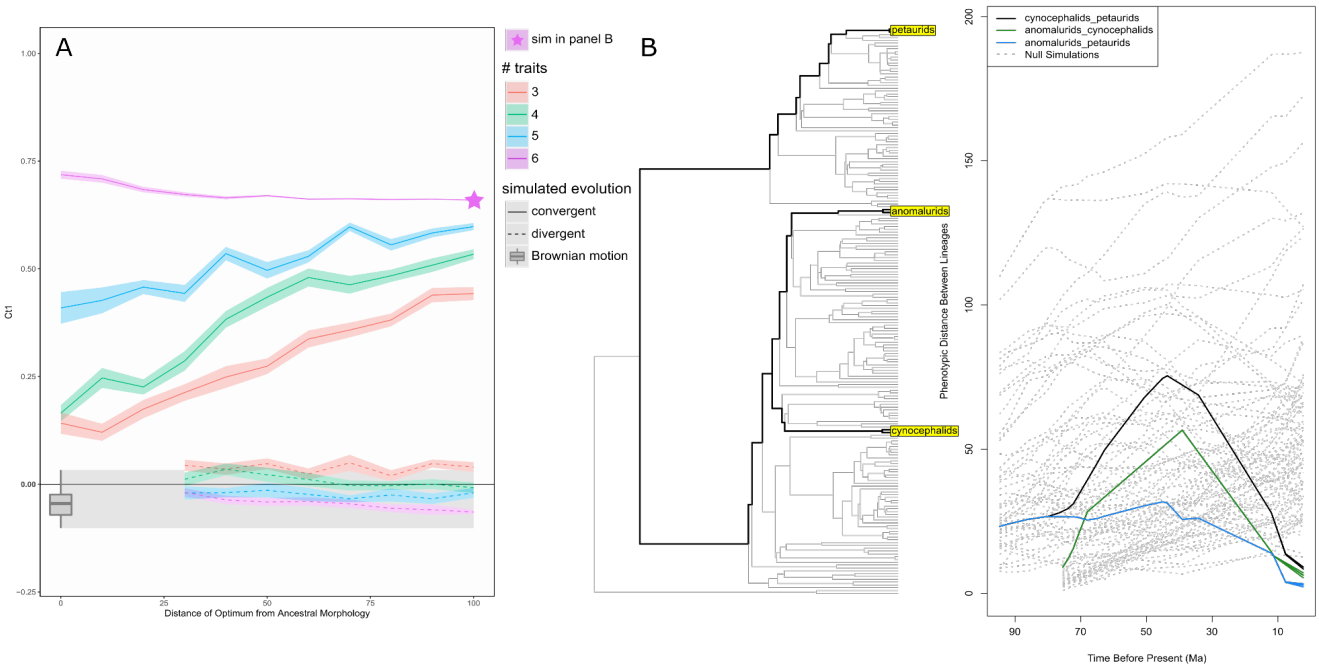

Figure 5. (*A*) *Ct*1 scores for simulated convergent lineages (top results in plot) and divergent lineages (bottom) under varying evolutionary scenarios. See the Methods and Figure 3 caption for more information. Although in some cases the divergence *Ct*1 results are greater than zero (indicating convergence), these results were not statistically significant when we calculated simulation-based *p*-values for a subset of datasets (Table 1). *C*1 results are means and standard errors of 15 simulated datasets. (*B*) An example output from the *plot.C* *R* function that shows the pairwise distances between lineages with time. Note that although only three 'glider' lineages are highlighted in the plot, five lineages were used for *Ct1* measurements.

We tested the performance of *Ct*-measures by applying them to the simulated datasets using the same methodology as that for *C*-measures. Unlike the *C*-measures (Fig. 3C), the *Ct*-measures do not consistently misidentify divergent lineages as being convergent (Figs. 5A and S2); most of the simulated divergence datasets (via both drift/BM and selection/OU) exhibit *Ct*1 scores that are negative, correctly indicating divergence. Like *C*-measures, the *Ct*-measures do measure more convergence in morphological outliers (Figs. 4A and 5A), but this pattern appears to be less pronounced than with *C*-measures (Figs. 2A and 3C). Although in some cases the *Ct*1 score is greater than zero (indicating convergence; Fig. 5A), the *Ct*1 scores are not statistically significant when applied to divergence datasets (Table 1), which is in contrast to the strongly significant *C*1 scores for divergence simulations. Further, the greater-than-zero *Ct*1 results could be due in part to convergence occasionally occurring by chance in our simulated-divergence datasets (e.g., BM-evolved 'glider' lineages evolving toward each other by chance). This indicates the importance of researchers considering the *p*-values associated with *Ct*-measures when evaluating convergence in their samples.

Different origination ages of convergent clades might also inflate *Ct* scores in morphological outliers, especially if the oldest lineage evolves rapidly into outlying morphospace and away from other putatively convergent lineages. This is illustrated in Figure S3 and discussed in the Supplemental Results. To help address this issue, we added an optional feature to the *convrat.t* function that limits candidate $D_{\mathrm{max.t}}$ measurements to the time prior to the evolution of the focal lineages (e.g., prior to the evolution of the earliest glider clade). We recommend that researchers use this option as a supplement to regular *Ct*-measures when their clades of interest have very different origination ages (see Supplemental Results).

Empirical examples – *C*1 vs *Ct*1

The *C*-measure issues highlighted here are relevant to the many studies that have employed (or will employ) the *C*-measures. In many cases, erroneous *C*-measure

results may have led researchers to either infer convergence in lineages that are divergent or infer inflated degrees of convergence. For instance, Grossnickle et al. (2020) tested for convergence among gliding mammal lineages using limb measurements, and they observed conflicting results. Statistically significant *C*-measure scores indicated strong convergence, but other analyses (evolutionary model-fitting, morphological disparity, phylomorphospace trajectories) suggested parallel evolutionary patterns. The authors concluded that the conflicting lines of evidence indicated weak, incomplete convergence. But considering the issues highlighted here, the strong *C*-measure results in Grossnickle et al. (2020) are probably misleading. For instance, the *C*-measure scores were likely inflated due to the outlying morphologies of some gliders (e.g., dermopterans), meaning that the gliders are probably less convergent than the authors concluded. We re-analyzed the data from Grossnickle et al. (2020) using the *Ct*-measures, and in contrast to strong *C*-measure scores, we found that all glider comparisons have negative *Ct*1 scores, indicating divergence instead of convergence. In some instances, the *Ct*1 scores are only slightly negative and have significant *p*-values (e.g., *Ct*1 = -0.01 and $p < 0.01$ for the comparison of scaly-tailed squirrels and flying squirrels), which is congruent with the other lines of evidence examined in Grossnickle et al. (2020) that suggested parallel evolutionary changes rather than convergence for most glider groups.

Huie et al. (2021) and Stayton (2015A; using data from Mahler et al. 2013) independently analyzed *Anolis* lizard morphologies using distinct datasets, and both found that the ecomorphotypes with the greatest *C*1 scores are those in the outermost regions of morphospace (‘crown-giant,’ ‘grass-bush,’ and ‘twig’; see Figure 3 of Huie et al. 2021). The *C*1 values for these ecomorphotypes ranged from 0.31 to 0.43 in these studies, whereas other, non-outlying ecomorphotypes had *C*1 values ranging from 0.09 to 0.25 (Stayton 2015A, Huie et al. 2021). The relatively large *C*1 scores of outlying ecomorphotypes, in addition to the positive *C*1 scores for all pairwise comparisons, may be due in part to the biases in the *C*-measure. We evaluated this possibility by applying *Ct*-measures to one of the outlying ecomorphotypes ('twig') from the anole dataset of Mahler et al. (2013; ten standardized skeletal measurements). We found that, although the overall *Ct*1 score was statistically significant, it was near zero (Table S2), in contrast

to the *C*1 score being 0.36 (Stayton 2015A). Interestingly, there was considerable
730 disparity in the pairwise *Ct* results for the five twig lineages, with *Ct*1 scores ranging
from 0.346 (*A. paternus* vs. *A. valencienni*) to -0.763 (*A. occultus* vs. *A. paternus*) and
732 six of ten pairwise comparisons not significant. (See Figure S5 and Table S2 for full
results and plotted pairwise distances through time.) Thus, these results highlight not
734 only the issues with the *C*-measures, namely the inflation of *C* scores among outliers,
but also the importance of considering pairwise comparisons when evaluating
736 convergence among multiple focal lineages.

738 ***Ct*-measures – recommendations and limitations**

In contrast to *C*-measures, the *Ct*-measures are influenced by the timing of evolutionary
740 change because they limit candidate $D_{max.t}$ measurements to specific time slices. This
feature should be considered by researchers who apply the *Ct*-measures because it
742 may alter expectations about the degree of measured convergence. For instance, if
different lineages of interest evolve toward a specific morphology (or adaptive peak) at
744 different points in time, then the $D_{max.t}$ measurement may not measure the
morphologically farthest distances between the lineages, possibly resulting in lower-
746 than-expected *Ct* scores. Conversely, and as noted above, if the putatively convergent
taxa evolve toward outlying regions of morphospace, then the asynchronous origins of
748 the clades could inflate the *Ct*-measures (Supplemental Results; Fig. S3). To help
mitigate this issue, we recommend that researchers generate and assess
750 phylomorphospace and distances-between-lineages-through-time plots, and compare
default *Ct* results to those generated when using the alternative option of the *convrat.t*
752 function that limits candidate $D_{max.t}$ measurements to the period in which lineages of
interest overlap in time (see Supplemental Methods).

754 The *Ct*-measures may perform poorly when the tips of focal taxa are very
different in geologic age (e.g., ichthyosaurs and dolphins) because candidate $D_{max.t}$
756 measurements are restricted to the period in which the lineages overlap in time. In the
case of ichthyosaurs and dolphins, their evolutionary histories overlap from their most
758 recent common ancestor (MRCA; early amniotes) to the ichthyosaur tips, so the
candidate $D_{max.t}$ measurements would be limited to between the MRCA and the

760 ichthyosaur tips. Thus, much of the evolutionary history of dolphins (and placental mammals more broadly) would be excluded by *Ct*-measures. This is likely to lead to
762 smaller-than-expected $D_{max.t}$ values because the morphological divergence of mammals from ichthyosaurs is not captured. Note, however, that D_{tip} ignores time and would
764 measure the morphological distance between ichthyosaur and dolphin tips.

The restriction of candidate $D_{max.t}$ measurements to coincide with internal nodes
766 exacerbates an issue inherent to many phylogenetic comparative methods: the reliance on inferred ancestral states. $D_{max.t}$ is the critical value that enables the *Ct*-measures to
768 diagnose convergence, and it is drawn entirely from ancestral state data, which are estimated from tip values assuming a BM model of evolution. The consequence is that
770 ancestral reconstructions are likely to reflect average morphologies of the sampled taxa, decreasing the chance of measuring convergence via the *Ct*-measures because $D_{max.t}$
772 estimates may be artificially shorter than the 'real' $D_{max.t}$ values. This is likely to be exacerbated under conditions where there are relatively few intervening nodes between
774 putatively convergent lineages (i.e., there is a small sample of candidate $D_{max.t}$ measurements), when those putatively convergent lineages are subtended by long
776 branches (i.e., distances from which to draw $D_{max.t}$ are biased toward deeper nodes), and when only contemporary tips are included (i.e., there is a lack of fossil data
778 informing reconstructions at internal nodes). Therefore, the *Ct*-measures may be most appropriate for well-sampled study systems that include a substantial number of internal
780 nodes and relatively few long branches, and researchers should include fossil taxa whenever possible to improve ancestral reconstructions at internal nodes.

782 The number of phenotypic traits used to assess convergence is likely of increased importance when using *Ct*-measures. In multivariate datasets, some traits
784 may be convergent and others non-convergent (i.e., divergent, parallel, or conservative). While including a greater number of non-convergent traits in analyses is
786 expected to decrease the overall convergence signal of any convergence measure, it may also exacerbate the *Ct*-related issues raised in this section. In general, adding
788 traits increases the measured distances between tips and internal nodes. However, ancestral inference via BM tends to average variation at internal nodes; thus, D_{tip}
790 typically increases at a higher rate than $D_{max.t}$ for each non-convergent trait that is

added to a dataset. This pattern is illustrated in Figure S4, highlighting that increasing
792 the number of BM-evolved traits (which are expected to be mostly non-convergent) in simulations results in relatively greater increases of D_{tip} scores compared to $D_{max.t}$
794 scores. Therefore, an increased number of traits in analyses (with all else equal) could result in a relative decrease in *Ct* scores compared to datasets with fewer traits, unless
796 the additional traits are strongly convergent. We recommend that researchers carefully choose traits (or landmarks if using geometric morphometrics) based on the specific
798 hypothesis being tested, and analyze individual traits or subsets of traits whenever feasible to tease apart unique patterns among traits.

800 Many of the aforementioned factors that could influence *Ct*-measures, especially the assumption of a BM mode of evolution in ancestral lineages, could contribute to the
802 *Ct*-measures being conservative in their measures of convergence. The conservative nature of the *Ct*-measures is supported by our simulation results; despite simulating
804 extremely strong convergence on a trait optimum for all six traits, the greatest *Ct*1 scores are around 0.7, indicating that about 70% of $D_{max.t}$ has been closed by
806 convergent evolution. Based on the simulation methods, we expected these values to be closer to 1.0. Thus, the convergence signal of *Ct*-measures might often be diluted
808 due to the issues noted here. This should be considered by researchers who use the *Ct*-measures.

810 As highlighted throughout this study, convergence measures can be biased based on the location of taxa in morphospace, with outliers tending to show greater
812 convergence when using the *C*-measures, *Ct*-measures (although to a lesser degree than *C*-measures), θ, and OU-model-fitting analyses, and less convergence when using
814 the Wheatsheaf index (Figs. 2A and 4A, Tables 1 and 2). We consider the greater observed convergence in morphological outliers via most methods to be an issue (Fig.
816 2A) because it is inconsistent with our working definition of convergence, which has the precision that allows for quantitative comparisons. However, under looser definitions of
818 convergence this pattern could be interpreted as a reflection of the amount of evolutionary change of the convergent lineages. Outliers have undergone greater
820 morphological change, evolving farther from the ancestral morphology, and thus their tendency to appear ‘convergent’ could be an emergent property of the evolution of

outlying morphologies (e.g., see Collar et al. [2014] for a discussion of 'imperfect convergence' in divergent, outlying lineages). This, however, is not what the measures of convergence have been defined to test, and we emphasize that researchers should ensure that their chosen convergence metrics and interpretations of results align with their *a priori* definition of convergence. In any case, researchers should expect to observe relatively stronger evidence of convergence in outliers when using most convergence measures.

Summary

The *C*-measures are a popular means of identifying and quantifying convergence, in part because they can differentiate between convergence and conservatism. However, we highlight a critical issue: *C*-measures can misidentify outlying, divergent lineages as convergent (Figs. 2 and 3, Table 1). OU-model-fitting analyses suffer from a similar issue because support for multiple-regime OU models over other models, which is often interpreted as evidence for convergence, can occur even when lineages are divergent, not convergent (Table 2). To help address this issue, we developed improved convergence measures (*Ct*-measures) that quantify distances between lineages at time slices at internal phylogenetic nodes, minimizing the possibility of divergent taxa being mistakenly measured as convergent. We have also developed new features (available in the *convevol R* package), such as a function to produce distances-between-lineages-through-time plots and the ability to compare clades that include multiple taxa. Although *Ct*-measures improve on *C*-measures, researchers should recognize their limitations. For instance, *Ct*-measures may be unreliable if convergent evolutionary change is asynchronous between lineages of interest (e.g., fossils of very different geologic ages), especially when lineages are morphological outliers. More broadly, we find that multiple methods (including *Ct*-measures) are biased by the location of taxa in morphospace, with most methods measuring greater convergence in morphological outliers. Because all available methods for identifying and measuring convergence are imperfect, we recommend that researchers use multiple convergence methods, incorporate fossils whenever possible to improve the accuracy of ancestral state reconstructions, and recognize the benefits and drawbacks of the chosen methods when interpreting results.

ACKNOWLEDGEMENTS

For helpful discussion and feedback, we thank Miriam Zelditch, Gregory Wilson Mantilla, Eli Amson, Kenneth-Dieter Benton, Allison Bormet, Richard Meyn, Sharlene Santana, and members of the 'Tempo & Mode in Isolation' discussion group. Jonathan S. Mitchell wrote the *R* script (published in Zelditch et al. 2017) that we adapted for the updated *convevol* functions, and we greatly appreciate his permission to use the code. Funding for D.M.G. was provided by National Science Foundation (NSF) grants DBI-1812126 and IOS-2017738. C. J. L. was funded by an Early Career Provost Fellowship at the University of Texas at Austin, the NSF (DBI−1906248 and DBI–2128146), the Gerstner Family Foundation, the Richard Gilder Graduate School, and the Department of Mammalogy at the American Museum of Natural History. L. N. W. was funded by the NSF Graduate Research Fellowship and NSF grant EAR-PF 2052992.

LITERATURE CITED

Akaike, H. 1974. A new look at the statistical model identification. IEEE Transactions on Automatic Control 19:716–723.

Alfieri, F., L. Botton-Divet, J. A. Nyakatura, and E. Amson. 2021. Integrative Approach Uncovers New Patterns of Ecomorphological Convergence in Slow Arboreal Xenarthrans. J. Mamm. Evol. 1-30.

Arbour, V. M., and L. E. Zanno. 2020. Tail Weaponry in Ankylosaurs and Glyptodonts: An Example of a Rare but Strongly Convergent Phenotype. Anat. Rec. 303:988–998.

Arbuckle, K., C. M. Bennett, and M. P. Speed. 2014. A simple measure of the strength of convergent evolution. Methods Ecol. Evol. 5:685–693.

Arbuckle, K., and Minter, A. 2015. Windex: Analyzing convergent evolution using the Wheatsheaf index in R. Evol. Bioinform. 11:EBO-S20968.

Beaulieu, J. M., D.-C. Jhwueng, C. Boettiger, and B. C. O'Meara. 2012. Modeling stabilizing selection: Expanding the Ornstein-Uhlenbeck model of adaptive evolution. Evolution 66:2369–2383.

Bollback, J. P. 2006. SIMMAP: stochastic character mapping of discrete traits on phylogenies. BMC Bioinformatics, 7:1–7.

Butler, M. A., and A. A. King. 2004. Phylogenetic Comparative Analysis: A Modeling Approach for Adaptive Evolution. Am. Nat. 164:683–695.

Baumgart, S. L., P. C. Sereno, and M. W. Westneat. 2021. Wing shape in waterbirds: morphometric patterns associated with behavior, habitat, migration, and phylogenetic convergence. Integr. Org. Biol. 3:obab011.

Canale, J. I., Apesteguía, S., Gallina, P.A., Mitchell, J., Smith, N.D., Cullen, T.M., Shinya, A., Haluza, A., Gianechini, F.A., Makovicky, P.J. 2022. New giant carnivorous dinosaur reveals convergent evolutionary trends in theropod arm reduction. Curr. Biol. 32:3195–3202.

Castiglione, S., G. Tesone, M. Piccolo, M. Melchionna, A. Mondanaro, C. Serio, M. De Febbraro, and P. Raia. 2018. A new method for testing evolutionary rate variation and shifts in phenotypic evolution. Methods. Ecol. Evol. 9:974–983.

Castiglione, S., C. Serio, D. Tamagnini, M. Melchionna, A. Mondanaro, M. De Febbraro, A. Profico, P. Piras, F. Barattolo, P. Raia. 2019. A new, fast method to search for morphological convergence with shape data. PLOS One 16:e0252264.

Clavel, J., G. Escarguel, and G. Merceron. 2015. mvMORPH: an R package for fitting multivariate evolutionary models to morphometric data. Methods Ecol. Evol. 6:1311–1319.

Collar, D. C., J. S. Reece, M. E. Alfaro, P. C. Wainwright, and R. S. Mehta. 2014. Imperfect morphological convergence: variable changes in cranial structures underlie transitions to durophagy in moray eels. Am. Nat. 183:E168–E184.

Cooper, N., Thomas, G. H., Venditti, C., Meade, A., & Freckleton, R. P. (2016). A cautionary note on the use of Ornstein Uhlenbeck models in macroevolutionary studies. *Biological Journal of the Linnean Society*, *118*:64–77.

Da Silva, F. O., A. C. Fabre, Y. Savriama, J. Ollonen, K. Mahlow, A. Herrel, J. Müller, and N. Di-Poï, N. 2018. The ecological origins of snakes as revealed by skull evolution. Nat. Commun. 9:1–11.

Darwin, C. 1859. *On the Origin of Species by Means of Natural Selection*. John Murray, London.

Drummond, A. J., M. A. Suchard, D. Xie, and A. Rambaut, 2012. Bayesian phylogenetics with BEAUti and the BEAST 1.7. Mol. Biol. Evol. 29:1969–1973.

Friedman, S. T., S. A. Price, A. S. Hoey, and P. C. Wainwright. 2016. Ecomorphological convergence in planktivorous surgeonfishes. J. Evol. Biol. 29:965–978.

Grossnickle, D. M. 2020. Feeding ecology has a stronger evolutionary influence on functional morphology than on body mass in mammals. Evolution 74:610–628.

Hansen, T. F. 1997. Stabilizing selection and the comparative analysis of adaptation. Evolution 51:1341–1351.

Huie, J. M., I. Prates, R. C. Bell, and K. de Queiroz. 2021. Convergent patterns of adaptive radiation between island and mainland *Anolis* lizards. Biol. J. Linn. Soc. Lond. 134:85–110.

Hurvich, C. M., and C. L. Tsai. 1989. Regression and time series model selection in small samples. Biometrika 76:297–307.

Ingram, T., and D. L. Mahler. 2013. SURFACE: detecting convergent evolution from comparative data by fitting Ornstein-Uhlenbeck models with stepwise Akaike Information Criterion. Methods Ecol. Evol. 4:416–425.

Law, C. J. 2022. Different evolutionary pathways lead to incomplete convergence of elongate body shapes in carnivoran mammals. Syst. Biol. 71:788-796.

Losos, J. B. 2011. Convergence, adaptation, and constraint. Evolution 65:1827–1840.

Mahler, D. L., T. Ingram, L. J. Revell, and J. B. Losos. 2013. Exceptional convergence on the macroevolutionary landscape in island lizard radiations. Science 341:292–295.

Mahler, D. L., M. G. Weber, C. E. Wagner, and T. Ingram. 2017. Pattern and process in the comparative study of convergent evolution. Am. Nat. 190:S13–S28.

Martinez, Q., J. Clavel, J. A. Esselstyn, A. S. Achmadi, C. Grohé, N. Pirot, and P. H. Fabre. 2020. Convergent evolution of olfactory and thermoregulatory capacities in small amphibious mammals. Proc. Natl. Acad. Sci. U.S.A 117:8958–8965.

McLean, B. S., K. M. Helgen, H. T. Goodwin, and J. A. Cook. 2018. Trait-specific processes of convergence and conservatism shape ecomorphological evolution in ground-dwelling squirrels. Evolution 72:473–489.

Pevsner, S. K., D. M. Grossnickle, and Z. X. Luo. 2022. The functional diversity of marsupial limbs is influenced by both ecology and developmental constraint. Biol. J. Linn. Soc. Lond. 135:569-585.

Polly, P. D. 2019. Phylogenetics for Mathematica. Version 6.5. Department of Earth and Atmospheric Sciences, Indiana University: Bloomington, Indiana. https://pollylab.indiana.edu/software.html.

R Core Team 2020. R: A language and environment for statistical computing. Vienna, Austria: R Foundation for Statistical Computing.

Rovinsky, D. S., A. R. Evans, and J. W. Adams. 2021. Functional ecological convergence between the thylacine and small prey-focused canids. BMC Ecol. Evol. 21:1–17.

Serio, C., P. Raia, and C. Meloro. 2020. Locomotory adaptations in 3D humerus geometry of Xenarthra: testing for convergence. Front. Ecol. Evol. 8:139.

Spear, J. K., and S. A. Williams. 2020. Mosaic patterns of homoplasy accompany the parallel evolution of suspensory adaptations in the forelimb of tree sloths (Folivora: Xenarthra). Zool. J. Linn. Soc. zlaa154.

Speed, M. P., and K. Arbuckle. 2017. Quantification provides a conceptual basis for convergent evolution. Biol. Rev. Camb. Philos. Soc. 92:815–829.

Stayton, C. T. 2008. Is convergence surprising? An examination of the frequency of convergence in simulated datasets. J. Theor. Biol. 252:1–14.

Stayton, C. T. 2015A. The definition, recognition, and interpretation of convergent evolution, and two new measures for quantifying and assessing the significance of convergence. Evolution 69:2140–2153.

Stayton, C. T. 2015B. What does convergent evolution mean? The interpretation of convergence and its implications in the search for limits to evolution. Interface Focus 5:20150039.

Stayton C. T. 2018. *Convevol: quantifies and assesses the significance of convergent evolution.* R package version 1.3. https:cran.r-project.org/package=convevol.

Tamagnini, D., C. Meloro, P. Raia, and L. Maiorano. 2021. Testing the occurrence of convergence in the craniomandibular shape evolution of living carnivorans. Evolution 75:1738–1752.

Upham, N., J. A. Esselstyn, and W. Jetz. 2019. Inferring the mammal tree: species-level sets of phylogenies for questions in ecology, evolution, and conservation. PLOS Biol. 17:e3000494.

Weaver, L. N., and D. M. Grossnickle. 2020. Functional diversity of small-mammal postcrania is linked to both substrate preference and body size. Curr. Zool. 66:539–553.

Zelditch, M. L., J. Ye, J. S. Mitchell, and D. L. Swiderski. 2017. Rare ecomorphological convergence on a complex adaptive landscape: Body size and diet mediate evolution of jaw shape in squirrels (Sciuridae). Evolution 71:633–649.

SUPPORTING INFORMATION

A cautionary note on using quantitative measures of phenotypic convergence

David M. Grossnickle, William H. Brightly, Lucas N. Weaver, Kathryn E. Stanchak, Rachel A. Roston, Spencer K. Pevsner, C. Tristan Stayton, P. David Polly, Chris J. Law

SUPPLEMENTAL METHODS

Univariate model-fitting analyses

One limitation of the *mvMORPH* multivariate models, which are used for our primary model-fitting analyses, is that they do not permit the evolutionary rate (σ) or strength of attraction to optima (α) to vary between the two selective regimes ('gliders' and 'non-gliders'). This likely results in poor model performance because the datasets were simulated such that 'gliders' and 'non-gliders' should have different rates and attraction strengths. For example, the 'non-gliders' are evolved by BM, and thus they are not expected to exhibit attraction to a trait optimum, whereas the convergent 'glider' lineages are expected to exhibit strong attraction due to being simulated by an OU process. Further, the phylogenetic half-life (ln(2)/α) of the 'glider' regime cannot be calculated independent of the 'non-glider' regime if the α parameter is uniform across both regimes, which is the case with the multivariate models.

Thus, we also fit seven univariate evolutionary models to the subset of simulated datasets, including several multiple-regime OU models that permit σ and α to vary between regimes. Using functions in the *OUwie R* package (Beaulieu et al. 2012), we fit these models to the first principal component (PC1) scores of a principal components analysis of the six simulated traits. The univariate models include uniform (or single-regime) BM and OU models, as well as a suite of multiple-regime OU models (i.e., 'OUM' models of Beaulieu et al. 2012). The OU2 model keeps α and σ constant for both

regimes, the OU2A model allows α (but not σ) to vary between regimes, the OU2V model allows σ^2 (but not α) to vary between regimes, and the OU2VA model allows both σ and α to vary between regimes. As with the multivariate analyses, all models were fitted across 10 'simmaps' for each of the 30 datasets and relative support for models was measured using AICcW.

We recognize that fitting models to PC scores can lead to biased results (Uyeda et al. 2015), and thus our univariate results should be considered with caution. However, we feel that using PC1 scores here is justified for two reasons. First, the alternative option is to fit models to each of the six simulated traits individually, but four of the traits are evolved via a strong OU process and two traits are evolved via BM (in our subset of datasets used in model-fitting analyses; see Methods), and thus the model-fitting results are expected to vary considerably between those two types of traits. PC1 provides a single value for which results can be more easily interpreted compared to results for the six traits. Second, our conclusions concerning the use of model-fitting analyses for testing for convergence are based entirely on the multivariate model-fitting analyses (see Results & Discussion), and thus the results of the univariate model-fitting analyses (which are congruent with the multivariate results; Tables 2 and S1) do not influence the broad conclusions of this study. The univariate model-fitting analyses are simply a supplemental analysis that provide a fitted α value and phylogenetic half-life for the 'glider' regime.

***Ct*-measures**

We used the *R* script from Zelditch et al. (2017) as a foundation for the updated functions for calculating *Ct*1–*Ct*4 and simulation-based *p*-values because they are computationally faster than the original *R* functions in the *convevol R* package (Stayton 2015, Stayton 2018). Note that the relevant *R* functions are titled *calcConv* (*C* calculations) and *convSig* (significance testing) in the *R* code of Zelditch et al. (2017), *convrat* and *convratsig* in the original *convevol R* package, and *convrat.t* and *convratsig.t* for our updated measures.

$D_{max.t}$ measurement. The primary change made by the *Ct*-measures in comparison to Stayton's (2015) original *C*-measures is the way in which $D_{\max}$ is defined.

Ct-measures were designed to ensure D_{max} (now referred to as $D_{max.t}$) was obtained
1048 from comparisons of synchronous time points along the evolutionary paths leading to
the putatively convergent taxa of interest. In this way it prevents the inflation of $D_{max.t}$
1050 that resulted from comparison of asynchronous nodes (e.g., tips and internal nodes)
which often occurred when using the original metrics on lineages with outlying
1052 morphologies (Figs. 3C and 4). Several modifications to the source *R* code were made
to facilitate this change. Candidate $D_{max.t}$ measurements for putatively convergent
1054 lineages are now measured at each internal node along the branch paths from the most
recent common ancestor (MRCA) of the lineages (e.g., see Figures 4 and 5B). At each
1056 of these points we extracted the phenotypic distance between lineages as the euclidean
distance between the ancestral reconstruction at the focal node and the coincident
1058 reconstruction along the branch path of the other lineage. Where this corresponds to a
point along a branch (which is most cases) the ancestral state is estimated using
1060 formula [2] from Felsenstein (1985), which allows ancestral states to be interpolated at
any point along a given branch from reconstructions at the branch's ancestral and
1062 descendant nodes. The code for this was largely repurposed from the *contMap* function
of the *phytools R* package (Revell 2012). If no contemporaneous point exists on the
1064 opposite path for a given internal node (e.g., when comparing extinct and extant taxa),
then a measurement is not taken at that node. All distances measured between paths
1066 are stored for each pair of user defined tips. $D_{max.t}$ is the maximum of these distance
values, but it is restricted to predate either focal tip (i.e., $D_{max.t}$ cannot equal D_{tip}).
1068 Restriction of $D_{max.t}$ to predate the focal tips means the minimum *Ct*1 value is no
longer set to zero as in the original *C1*-measure. This allows for some degree of
1070 divergence to be captured (i.e., relatively more negative *Ct*1 values may represent
greater divergence). However, users are cautioned from using this to test the magnitude
1072 of divergence between clades. This is because in divergent clades $D_{max.t}$ will almost
always be the last time point before the oldest focal tip. The method will thus reflect only
1074 a small portion of the period when lineages were undergoing divergent evolution.
Degree of divergence will then be a function of both phenotypic rates of evolution and of
1076 subtending branch length. The latter will in many practical situations be a function of
sampling, with long subtending branches due to poor sampling likely to inflate

divergence measures substantially since they will provide the best scenario for a large time difference between D_{max} and D_{tip} (and thus capture the greatest proportion of divergent evolution).

The changes to D_{max} were the most consequential of those made to modify the original *C*-measures. However, a number of other new options were also included. These are briefly described below. Full documentation of these options will be available as part of the next update to the *convevol R* package (Stayton, 2018).

User-defined groups. The first new option is for users to provide grouping assignments to the tips being tested, thus allowing comparisons of clades with multiple lineages, whereas the original *C*-measures are limited to comparisons of individual lineages. This option removes pairwise comparison between tips within the same group (e.g., two flying squirrels would not be compared if all flying squirrels are defined as one group) and returns results for each unique comparison between groups in addition to overall results. This option is useful if it is hypothesized that two (or more) clades converged, and relieves the user from needing to average tip values of a clade or manually define all of the desired comparisons. When using this option, the overall (for all pairwise comparisons) and comparison-specific *Ct* and *p* values are returned. Overall results are provided as both raw values (means of all pairwise comparisons, excluding within-group comparisons) and weighted values. The latter allows each inter-group comparison to impact the overall average equally, so that larger within group sample sizes don't skew overall results. For instance, if there are three putatively convergent groups (Group A, Group B, and Group C), and Groups A and B both include a single lineage and Group C includes 10 lineages, then there would be 21 total pairwise comparisons among groups (one for A-B, 10 for A-C, and 10 for B-C). Although constituting one third of the unique inter-group comparisons, *Ct* measurements taken from comparison of Groups A and B constitute less than 5% of those used to compute overall (average) *Ct* values. Thus, Groups A and B have a relatively smaller impact than Group C on the overall *Ct* scores and *p*-values. The weighted output scales the *Ct* results (and associated *p*-values) so that each unique inter-group comparison contributes equally to the overall results, whereas the raw overall result simply reports the mean value for all 21 pairwise comparisons. Both weighted and unweighted values

are reported in the default output printed by the updated *convSig* function, but we
1110 recommend the weighted result be used by default when comparing groups.
Nevertheless, the raw result may be preferable in cases in which researchers believe
1112 that the more heavily sampled group(s) should have a larger impact on overall results.

Note that it is possible to define groups even when those consist of a single tip.
1114 While doing so will not change which pairwise comparisons the model considers, it will
provide the user with unique *Ct* scores and *p*-values for each comparison. This can be
1116 especially useful when the degree of convergence varies across the lineages of interest
(e.g., see the pairwise results for anole species in Figure S5 and Table S2).

1118 *Conservative $D_{max.t}$ option.* When providing user-defined groups, a conservative
$D_{\mathrm{max.t}}$ option is available that limits candidate $D_{\mathrm{max.t}}$ measurements to a time point
1120 predating the origination of both focal groups (i.e., the nodes of the MRCAs of each
group). This is to prevent $D_{\mathrm{max.t}}$ being skewed by an early transition of one lineage
1122 toward a shared adaptive optimum that is outlying in morphospace, which can result in
inflated *Ct* scores, especially when the origins of the clades are very different in age.
1124 This issue is discussed in the Supplemental Results and illustrated in Figure S3. Note
that this option is only meaningful when user defined groups are provided. When one of
1126 those groups consist of a single lineage the node immediately ancestral to the tip is
used. Using this method, long branches can substantially alter inferred $D_{\mathrm{max.t}}$ values. We
1128 have provided the option to print relevant information about the restrictions put on $D_{\mathrm{max.t}}$
when using this method (by setting VERBOSE = TRUE in *convrat.t*). We strongly
1130 suggest that users investigate the impact of using the conservative $D_{\mathrm{max.t}}$ option before
committing to significance tests.

1132 *Updated Ct4 computation.* In addition to changes to $D_{\mathrm{max.t}}$, we also altered the
way in which the *C*4-measure is computed. The new version (called *Ct*4) redefines
1134 $L_{\mathrm{tot.clade}}$, which is the value used to standardize the *C*2 value (D_{max} subtracted by D_{tip}) to
obtain *C*4. $L_{\mathrm{tot.clade}}$ is described by Stayton (2015) as reflecting the total amount of
1136 morphological evolution which occurs in the clade originating with the MRCA of two
putatively convergent tips. In the original *C*-measures, $L_{\mathrm{tot.clade}}$ values were obtained as
1138 a sum of the phenotypic distances from all pairwise comparisons between nodes in the
clade, but this does not fully account for phylogenetic structure and is heavily influenced

by sampling intensity. We have updated this to now be the sum of the phenotypic distances accumulated along each branch in the clade of interest. This change brings *C*4 closer to the original description of the metric.

Measuring convergence of single traits. By default, the original *C*-measures do not support investigation of convergence in a single trait (although see Spear and Williams, 2020; Law, 2022). To circumvent this limitation we have added code to the *convrat.t* function which appends an invariant trait (with value zero) to datasets consisting of a single trait. This approach was taken due to ease of integration with existing code, and although crude will provide the same phenotypic distances as would be obtained from the single trait.

Model output. Additional changes were made to increase the amount of information returned to the user and facilitate plotting of results. This includes the addition of the novel *plot.C* function, which is described in the 'Measuring convergence through time via Ct-measures' section of the main text (with example output in Figure 5B).

SUPPLEMENTAL RESULTS

Univariate model-fitting analyses

For univariate models fit to PC1 scores the OU2VA model, which allows varying rates and attraction strengths between regimes, is the best fitting model at all trait optimum values for both convergence and divergences datasets (Table S1). However for convergence datasets, the null model (BM1) is the second best-fitting model when the trait optimum is zero and 20, and the total AICcW values for all OU2 models increases with greater optima values, indicating increased evidence of convergence in morphological outliers. These results are consistent with the results of the multivariate evolutionary models (Table 2).

Table S1. Tests of convergence among lineages of the simulated datasets using evolutionary models fit to univariate data (PC1 scores). Model-fitting results for each trait optimum are the mean AICcWs of 50 phylogenetic trees (five datasets with 10 'simmaps' each). Model support for the two-regime models (any variation of the OU2 model) could be interpreted as support for convergence because this model reflects evolution of the putatively convergent lineages toward a shared adaptive peak (but see the Results & Discussion). Abbreviations: AICcW, small-sample corrected Akaike weights; BM, Brownian motion; OU, Ornstein-Uhlenbeck.

	Model	**Trait optimum**			
		0	**20**	**50**	**100**
Convergence simulations	BM1	0.157	0.043	0.000	0.000
	OU1	0.058	0.015	0.000	0.000
	OU2	0.041	0.020	0.001	0.000
	OU2A	0.016	0.014	0.103	0.338
	OU2V	0.058	0.022	0.023	0.000
	OU2VA	0.670	0.885	0.873	0.661
Divergence simulations	BM1	–	–	0.000	0.000
	OU1	–	–	0.000	0.000
	OU2	–	–	0.000	0.000
	OU2A	–	–	0.116	0.331
	OU2V	–	–	0.001	0.020
	OU2VA	–	–	0.882	0.649

In the main text, we discuss a few factors that likely explain why the two-regime OU models are unexpectedly the best-fitting models to divergent data. Namely, the two-regime OU may be the best-fitting of bad-fitting models, with the BM1 and OU1 models even worse fits to the data. An additional factor that may contribute to the relatively strong fits of two-regime OU models to divergence datasets is that we treated the datasets as we would with empirical datasets and used 'simmaps' for ancestral state reconstructions of regime states (gliding or non-gliding), rather than use the known node information (via the simulation data). For instance, the two marsupial glider groups in our dataset are closely related (but believed to have evolved gliding independently), and

thus the ‘simmaps’ might commonly (and mistakenly) reconstruct the MRCA of those lineages as having gliding behavior.

***C*1–*C*4 and *Ct*1–*Ct*4 applied to simulated data**

In the main text we only present results for *C*1 (Fig. 3C, Table 1) and *Ct*1 (Fig. 5A, Table 1), which were applied to both the simulated convergence datasets and the simulated divergence datasets. However, Stayton (2015) developed four distance-based convergence measures (*C*1–*C*4) and one frequency-based measure (*C*5), with *C*1 being the primary measure, and we altered *C*1-*C*4 to produce the *Ct*1–*Ct*4 measures. Here, we provide full results for *C*1–*C*4 (Fig. S1) and *Ct*1–*Ct*4 (Fig. S2), which are also applied to both the convergence and divergence datasets. See the Methods and Stayton (2015) for descriptions of the four convergence measures, and see the Methods for information on the simulated datasets. Note that the *Ct*4 measure is calculated differently than the *C*4 measure (see Supplemental Methods). For *C*1–*C*4, all results for divergence simulations are greater than zero (Fig. S1), incorrectly indicating convergence, whereas the *Ct*1–*Ct*4 scores for divergence datasets are generally at or below zero (Fig. S2).

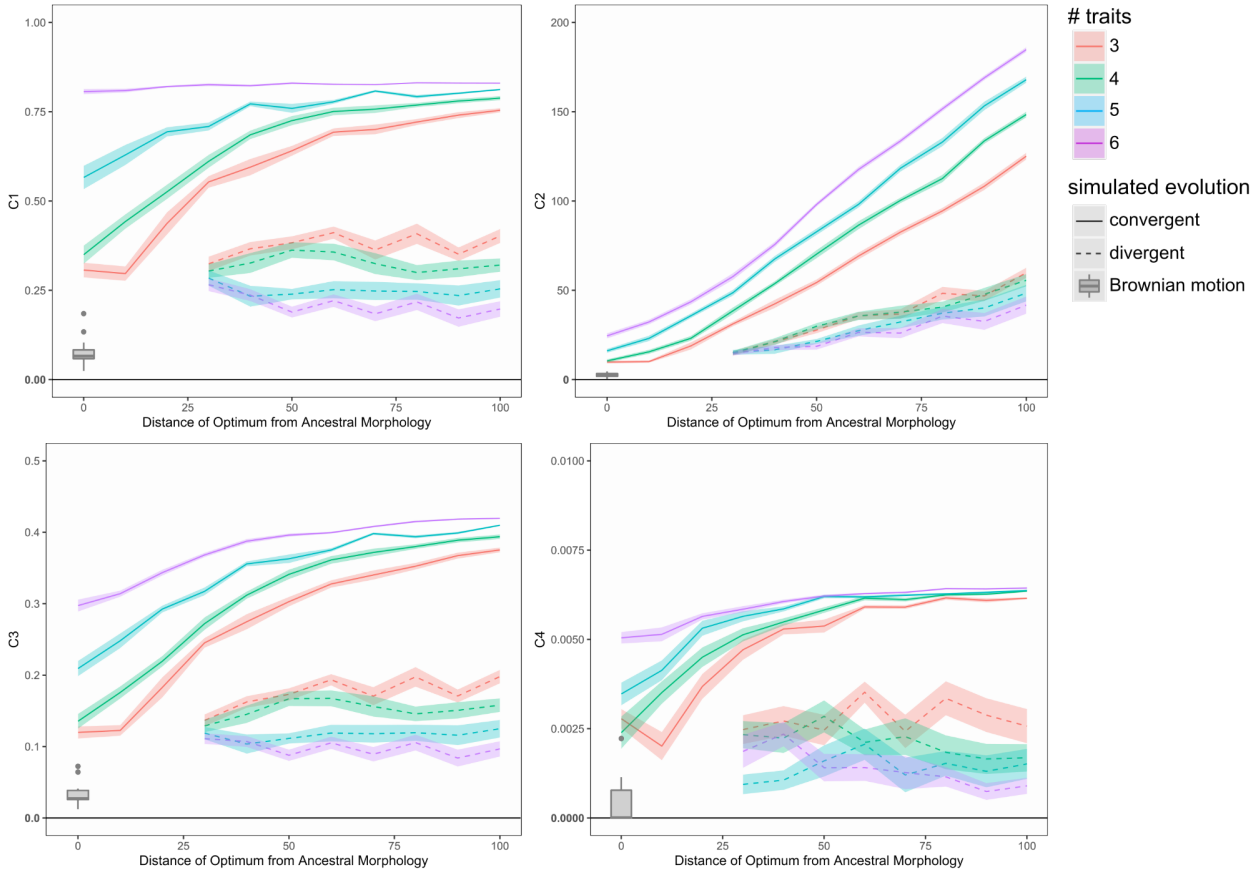

Figure S1. Plots of means and standard errors of *C*1–*C*4 scores for simulated convergent lineages (solid lines) and divergent lineages (dashed lines). Datasets varied in the number of convergent/divergent traits (represented by the different colored lines) and in the distance of trait optima from the ancestral morphology (approximated as the center of morphospace). Means and standard errors are computed from 15 simulated datasets. Greater *C*1–*C*4 values indicate greater convergence. We did not simulate divergence for trait optima of 0, 10, and 20 because at these optima our simulation methods may have inadvertently generated convergence patterns (see Methods and Figure 3). As a second means of simulating divergence, we allowed the lineages of interest ('gliders') to evolve via BM. These are provided as box-and-whisker plots, summarizing 15 simulated datasets of six traits (see Methods). Note that the divergence results are all greater than zero, incorrectly indicating convergence.

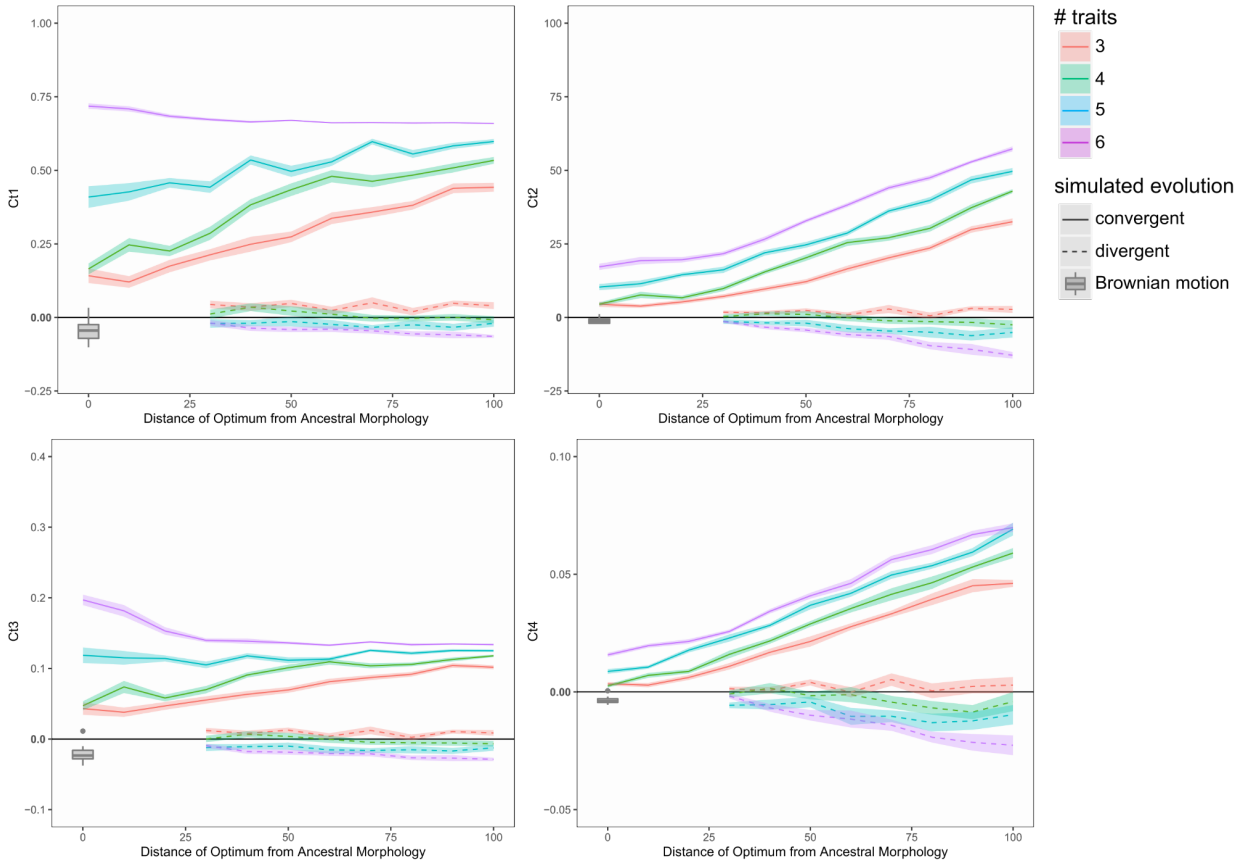

Figure S2. Plots of means and standard errors of *Ct*1–*Ct*4 scores for simulated convergent lineages (solid lines) and divergent lineages (dashed lines). Datasets varied in the number of convergent/divergent traits (represented by the different colored lines) and in the distance of trait optima from the ancestral morphology (approximated as the center of morphospace). Means and standard errors are each computed from 15 simulated datasets. Greater *Ct*1–*Ct*4 values indicate greater convergence. We did not simulate divergence for trait optima of 0, 10, and 20 because at these optima our simulation methods may have inadvertently generated convergence patterns (see Methods and Figure 3). As a second means of simulating divergence, we allowed the lineages of interest ('gliders') to evolve via BM. These are provided as box-and-whisker plots, summarizing 15 simulated datasets of six traits (see Methods). Note the differences in the scaling of the vertical axes of the *Ct*2 and *Ct*3 plots relative to the *C*2 and *C*3 plots (Fig. S1), respectively. (The scaling for *C*4 and *Ct*4 is different because these measures are calculated differently.) Also, note the different position of zero relative to results in the *Ct*1–*Ct*4 plots versus the position in *C*1–*C*4 plots (Fig. S1), as well as the overlap in the *Ct*1–*Ct*4 plots of divergence data simulated by both BM and OU processes.

***Ct*-measures – the influence of origination times on results**

As discussed in the main text, the *Ct*-measures limit candidate $D_{max.t}$ measurements to specific time slices at internal nodes, and thus the timing of evolutionary change among putatively convergent lineages can influence the results of *Ct*-measures. For instance, if different lineages of interest evolve toward (or away from) a specific morphology at different points in time, then the $D_{max.t}$ measurement may not measure the morphologically farthest distances between the lineages. This issue may be magnified when convergence is expected to be linked to adaptive changes (e.g., adaptations for gliding behavior) that evolved at specific times. For instance, if colugos (i.e., Dermoptera or 'flying lemurs') evolved traits associated with gliding behavior approximately 60 Ma, and flying squirrels (Pteromyini) evolved traits associated with gliding approximately 25 Ma (e.g., Grossnickle et al. 2020), then most of the candidate $D_{max.t}$ measurements will be comparisons of dermopterans with gliding traits to stem flying squirrels without gliding traits (from 60 to 25 Ma). If the older lineage (colugos) has already undergone considerable evolutionary change by the time that the younger lineage (flying squirrels) originated, then much of the convergent evolutionary change of the older lineage is not captured by the morphological distances measured at 'time slices,' which are limited to the time period in which the lineages overlap. Ideally, most candidate $D_{max.t}$ measurements would be comparisons of non-gliding stem colugos and non-gliding stem flying squirrels that lack the adaptive traits associated with gliding. This issue might lead to candidate $D_{max.t}$ measurements being smaller than expected, or at least smaller than those calculated by measures that ignore time (e.g., *C*-measures).

Conversely, if the putatively convergent taxa evolve toward outlying regions of morphospace, then the asynchronous origins of the clades could inflate the *Ct*-measures. We illustrate this in Figure S3. In the conceptual illustrations, the *Ct*1 score is consistently 0.3 when convergent lineages originate at the same time and/or when lineages evolve toward the ancestral morphology. However, when lineages originate at different times and evolve toward an outlying region of morphospace, then the *Ct*1 score is 0.7. Thus, researchers should be cautious when applying Ct measures to datasets with outlying taxa of various origination ages, and we offer some suggestions in the main text for mitigating this issue. It is also worth noting that this latter scenario

assumes that the convergent lineages can reach adaptive zones; if the later-evolving convergent lineage is still evolving toward outlying morphospace (i.e., it has yet to reach an adaptive peak or zone) then the aforementioned issue may have less of an influence on *Ct* results.

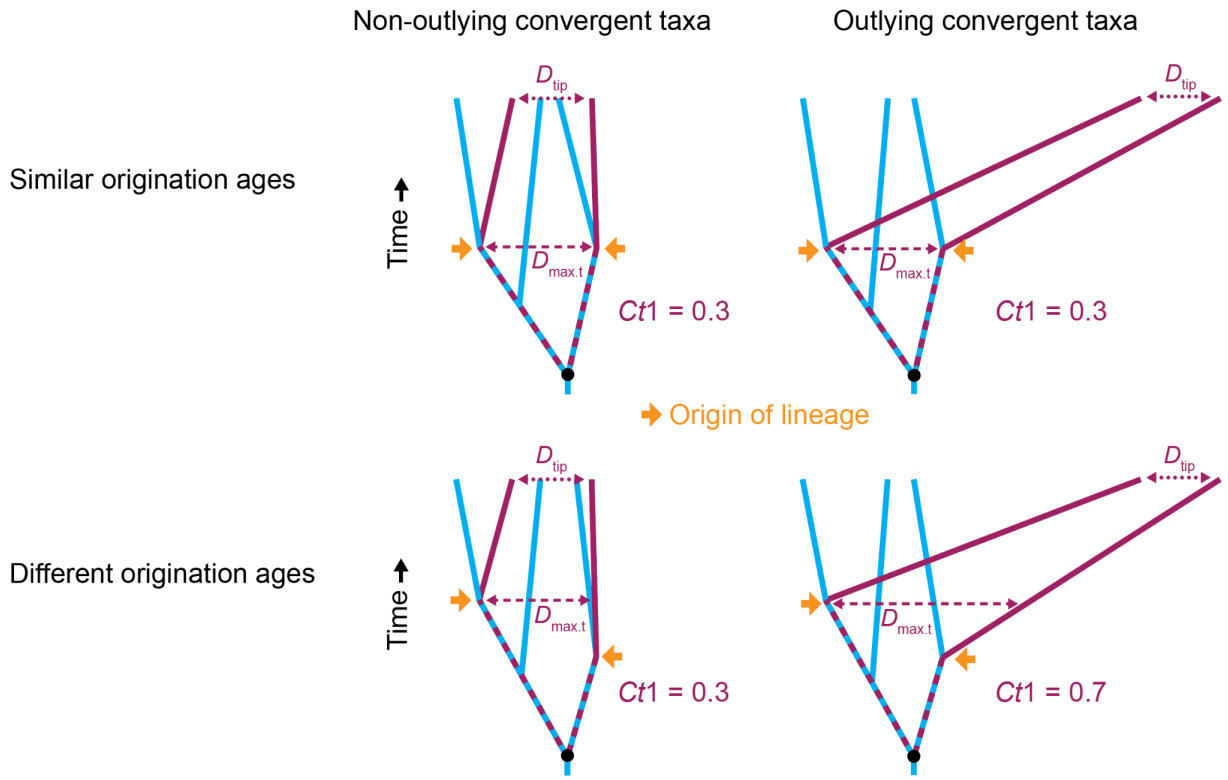

Figure S3. Conceptual illustrations demonstrating how *Ct*1 results can be influenced by a combination of outlying morphologies and varying origination times among convergent lineages. The *Ct*1 score is 0.3 in three of the scenarios but inflates to 0.7 when lineages both originate at different times and are outliers in morphospace (bottom right). To help mitigate this issue, we have included an option as part of the *convrat.t* function that allows users to limit candidate $D_{max.t}$ measurement to the time period prior to the origination of the focal lineages (see Supplemental Methods). See the main text for descriptions of *Ct*1, $D_{max.t}$, and D_{tip}.

Influence of the number of traits on *Ct* results

As discussed in the main text (see Results & Discussion), the number of traits used in analyses (with all else equal) can bias the *Ct* scores. Inference of ancestral states via BM tends to average variation at internal nodes; thus, D_{tip} typically increases at a higher rate than $D_{max.t}$ for each non-convergent trait that is added to a dataset. (Here, we use "non-convergent traits" to refer to BM-evolved traits that are not selected to evolve toward a trait optimum via an OU process. These are often divergent, although it should be noted that BM-evolved traits could still be convergent by chance.) This is illustrated in Figure S4. The effect of this pattern is that an increased number of traits in analyses (with all else equal) could result in a relative decrease in *Ct* scores, unless those added traits are strongly convergent.

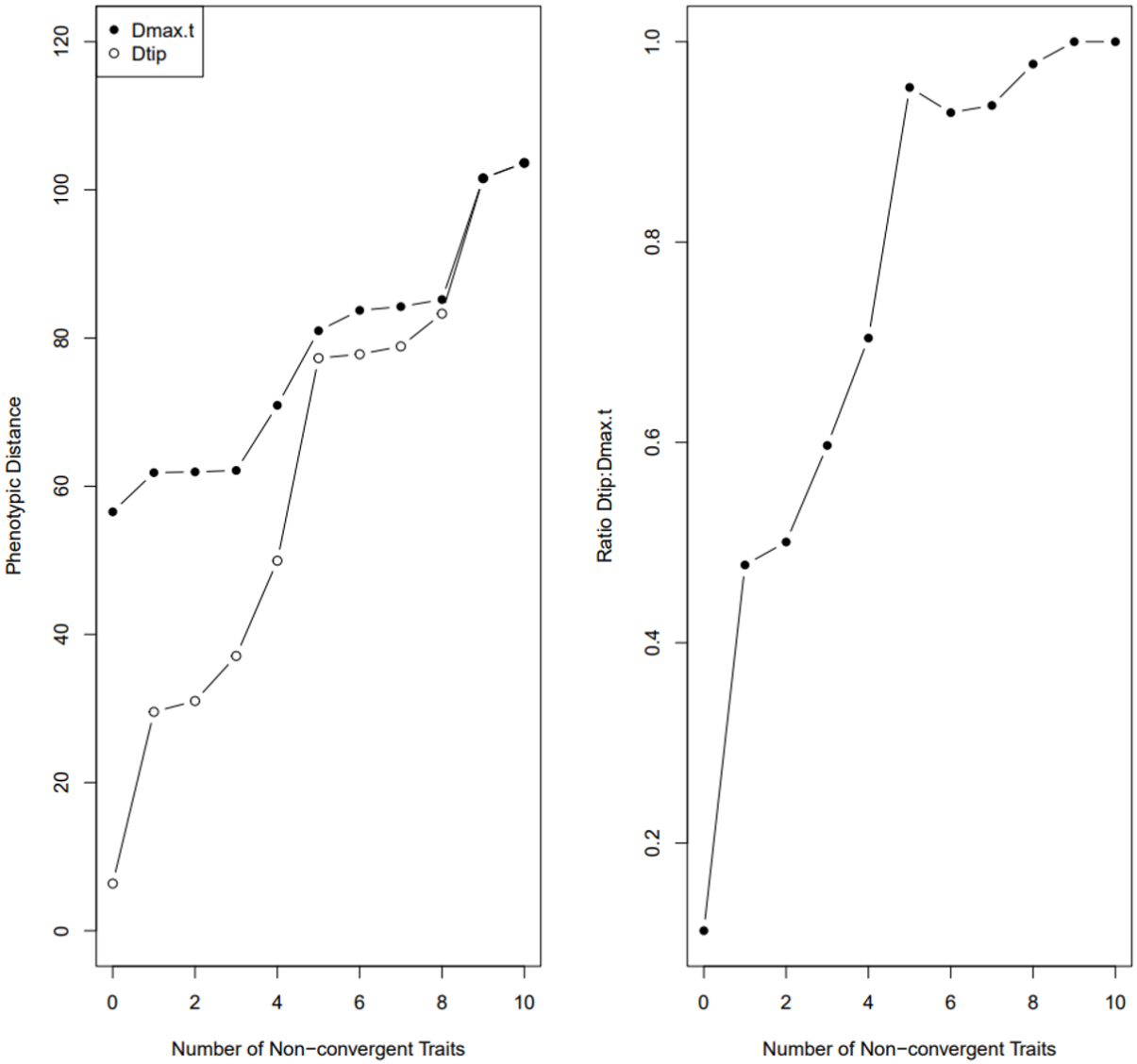

Figure S4. Illustration of how the number of traits used in analyses can influence *Ct*-measures, demonstrating the increased rate at which D_{tip} values increase relative to $D_{max.t}$ as additional non-convergent traits are included in analyses. (Here, 'non-convergent traits' refers to BM-evolved traits, which are expected to be divergent in most cases.) The left panel shows D_{tip} and $D_{max.t}$ measured between two 'glider' lineages with two simulated convergent traits (optimum = 100) and varying number of additional traits simulated via BM. The right panel shows the ratio between the D_{tip} and $D_{max.t}$ values.

Empirical example - *Anolis* 'twig' ecomorphotype

To test the novel *Ct*-measures and compare *Ct* results to those of *C*-measures (see the *Empirical examples* subsection of the Results & Discussion), we re-analyzed a classic example of convergence among *Anolis* lizards (Mahler et al. 2013), focusing specifically on five 'twig' ecomorphotype lineages. We chose this ecomorphotype because the taxa are morphological outliers that occupy a unique region of *Anolis* morphospace (Huie et al. 2021), and they have especially strong *C*-measure scores (Stayton 2015, Huie et al. 2021), although we believe that this is due in part to the lineages being morphological outliers (see Results & Discussion). Following the methods of Mahler et al. (2013), we size-corrected the traits via PGLS regression of each trait against the snout-to-vent length via PGLS. The *Ct*-measure results for this analysis are provided in Figure S5 and Table S2. Whereas the *C*1 score is 0.36 (Stayton 2015), but we find the overall *Ct*1 score to be near zero for both the raw and weighted results (Table S2). This helps to highlight the inflated *C*-measure results due to the issues highlighted in the Results & Discussion. However, note that there is considerable diversity in the results among the ten pairwise comparisons; four are strongly statistically significant, whereas some (e.g., *Anolis occultus* and the *A. paternus* clade) show considerable divergence (*Ct*1 = -0.763; Table S2). To highlight the differences between convergent and non-convergent (or not significant convergence) pairwise comparisons, we separate those comparisons in Figure S5. Thus, we recommend that researchers examine and report results for pairwise comparisons whenever examining more than two putatively convergent lineages.

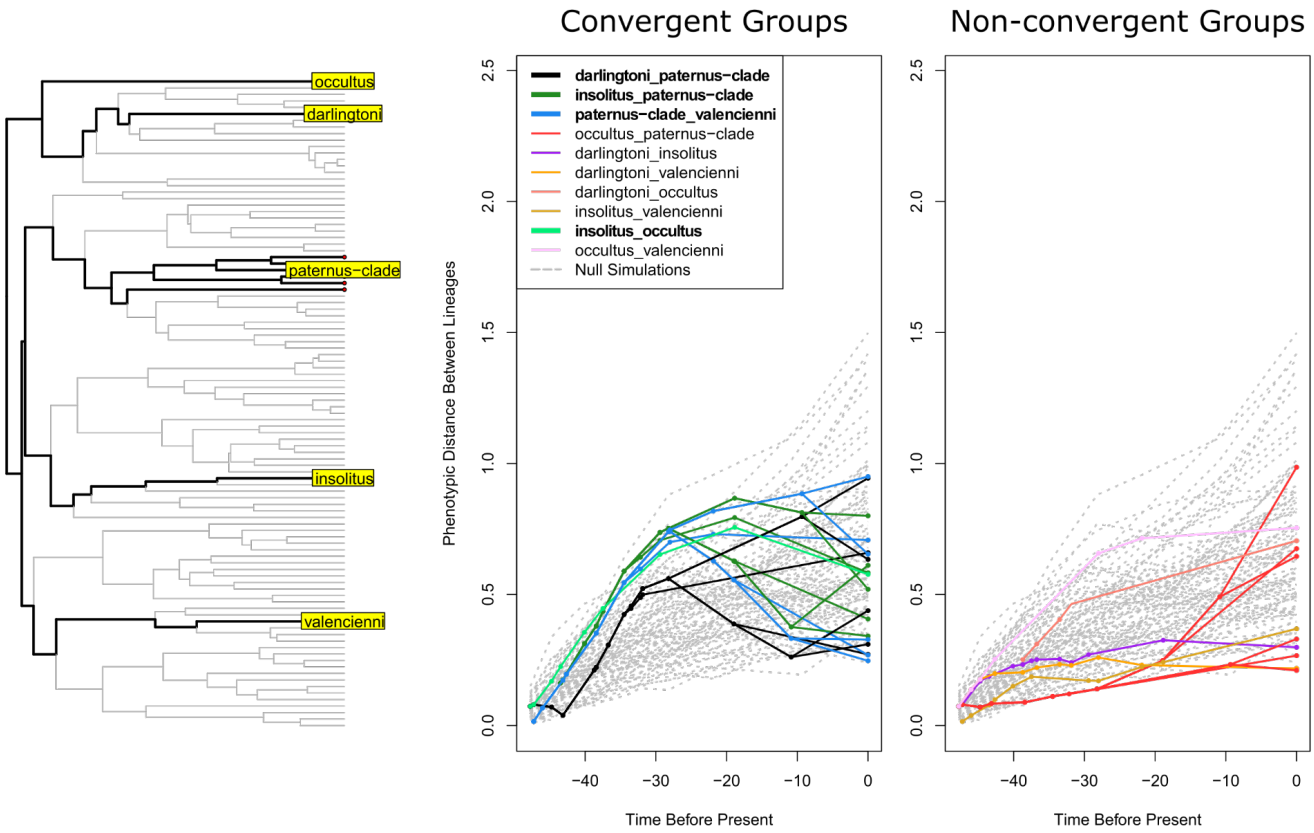

Figure S5. Summary of empirical tests of convergence in *Anolis* species belonging to the 'twig ecomorph' (Mahler et al. 2013). We size-corrected (via PGLS regression) and then analyzed the ten skeletal traits of the dataset of Mahler et al. (2013), with taxa assigned to groups based upon unique origins of the 'twig' ecomorphotype (see the *Ct-measures* section of the Supplemental Methods). The plots are the output of the *plot.C* function of the convevol R package, although the distance-through-time plot has been split to show statistically significant (left) and not significant (right) pairwise comparisons separately (see also Table S2). Significant pairwise comparisons are also indicated in bold in the key. Note that two of the 'non-convergent' comparisons in the right panel do have a positive *Ct*1 value, but they are statistically not significant (Table S2). There are 50 null simulations (light gray lines).

Table S2. *Ct*-measure values obtained for analyses run using the anole dataset of Mahler et al. (2013; ten standardized skeletal traits). Values are reported for overall comparison of ten'twig ecomorph' species in five groups (corresponding to each independent origin of the ecomorph; Fig. S5). Pairwise comparisons of groups are also illustrated in (Fig. S5). See the Supplemental Methods for an explanation of the difference between 'overall raw' and 'overall weighted' results. Note that 'pat' refers to a five-species clade that includes *Anolis paternus* and four closely related species, whereas all other 'twig' taxa include a single lineage (Fig. S5); see the Methods for updates to the *convevol R* package that allow for comparisons among taxa with more than one lineage. Asterisks denote values returned as significantly different from null simulations (. - p < 0.1, * - p < 0.05, ** - p < 0.01). Abbreviations: *dar, Anolis darlingtoni*; *ins, Anolis insolitus*; *occ, Anolis occultus*; *pat, Anolis paternus*; *val*, *Anolis valencienni*.

	Overall		Pairwise comparisons									
	Raw	**Weighted**	***dar - pat***	***ins - pat***	***pat - val***	***occ - pat***	***dar - ins***	***dar - val***	***dar - occ***	***ins - val***	***ins - occ***	***occ - val***
***Ct* 1**	-0.01**	-0.057**	0.147**	0.323**	0.346**	-0.763	0.083 .	0.161 .	-0.521	-0.527	0.237**	-0.055
***Ct* 2**	0.072**	0.022**	0.086**	0.254**	0.261**	-0.216	0.027 .	0.042 .	-0.241	-0.127	0.179**	-0.039
***Ct* 3**	0.039**	0.012**	0.047**	0.111**	0.140**	-0.090	0.013 .	0.023 .	-0.117 .	-0.063	0.071*	-0.018
***Ct* 4**	0.002**	-0.006 .	0.003**	0.019**	0.011**	-0.007	0.001 .	0.001 .	-0.089	-0.005	0.006**	-0.001

LITERATURE CITED (in the Supporting Information)

Beaulieu, J. M., D. C. Jhwueng, C. Boettiger, and B. C. O'Meara. 2012. Modeling stabilizing selection: expanding the Ornstein–Uhlenbeck model of adaptive evolution. Evolution 66:2369–2383.

Felsenstein, J. 1985. Phylogenies and the comparative method. Am. Nat. 125:1–15.

Huie, J. M., I. Prates, R. C. Bell, and K. de Queiroz. 2021. Convergent patterns of adaptive radiation between island and mainland *Anolis* lizards. Biol. J. Linn. Soc. Lond. 134:85–110.

Mahler, D. L., T. Ingram, L. J. Revell, and J. B. Losos. 2013. Exceptional convergence on the macroevolutionary landscape in island lizard radiations. Science 341:292–295.

Revell, L. J. 2012. phytools: an R package for phylogenetic comparative biology (and other things). Methods Ecol. Evol. 3:217–223.

Stayton, C. T. 2015. The definition, recognition, and interpretation of convergent evolution, and two new measures for quantifying and assessing the significance of convergence. Evolution 69:2140–2153.

1416 Stayton C. T. 2018. *Convevol: quantifies and assesses the significance of convergent evolution.* R package version 1.3. https:cran.r-project.org/package=convevol.

1418 Uyeda, J. C., D. S. Caetano, and M. W. Pennell. 2015. Comparative analysis of principal components can be misleading. Syst. Biol. 64:677–689.